Carcinogenesis vol.28 no.10 pp.2199–2206, 2007
doi:10.1093/carcin/bgm118
Advance Access publication May 16, 2007

Significance of inflammation-associated regenerative mucosa characterized by Paneth cell metaplasia and β-catenin accumulation for the onset of colorectal carcinogenesis in rats initiated with 1,2-dimethylhydrazine

Toshio Imai*, Katsuhiro Fukuta[1], Mai Hasumura, Young-Man Cho, Yoshio Ota, Shigeaki Takami, Hitoshi Nakagama[1] and Masao Hirose

Division of Pathology, National Institute of Health Sciences, 1-18-1 Kamiyoga, Setagaya-Ku, Tokyo 158-8501, Japan and [1]Biochemistry Division, National Cancer Center Research Institute, 1-1 Tsukiji, 5-chome, Chuo-ku, Tokyo 104-0045, Japan

*To whom correspondence should be addressed. Tel: +81 3 3700 9845; Fax: +81 3 3700 1425; Email: imai@nihs.go.jp

Short-term dextran sodium sulfate (DSS) treatment has been shown to notably accelerate colorectal tumor development in rats initiated with 1,2-dimethylhydrazine (DMH). In the present study, to clarify mechanisms underlying the DSS influence, time-course studies of histopathological and immunohistochemical characteristics and β-*catenin* gene mutations in colorectal mucosa in early stages of this model were conducted. F344 males were given three subcutaneous injections of DMH (40 mg/kg body wt) within a week, followed by free access to drinking water containing 1% DSS for a week. At weeks 1, 4, 6 and 8 after the DSS treatment, rats were euthanized and colorectal samples were collected. At week 1, the colorectal mucosa demonstrated extensive erosion along with significant inflammatory cell infiltration and neighboring reactive hyperplasia. By week 4, the mucosal damage was repaired and regenerative mucosa, partly characterized by Paneth cell metaplasia and altered subcellular localization of β-catenin, was apparent. Areas with Paneth cells/β-catenin accumulation were significantly more likely to be accompanied by interstitial inflammation and 17 of 24 dysplastic foci were found in regenerative mucosa with Paneth cells. Furthermore, adenomas/carcinomas frequently featured various degrees of Paneth cell differentiation. Point mutations mainly in codons 34 and 41 of β-*catenin* gene were detected in 6 of 27 samples of regenerative mucosa with Paneth cells and four of nine dysplastic foci/adenomas/carcinomas. These findings indicate that inflammation-associated regenerative mucosa with Paneth cell metaplasia and alteration in the APC/β-catenin/Tcf signal transduction pathway are possibly involved in the acceleration of colorectal carcinogenesis in this DMH–DSS rat model.

Introduction

Patients with chronic inflammatory bowel disease (IBD), which includes Crohn's disease and ulcerative colitis (UC), are at increased risk of developing colorectal cancer (1,2). Most IBD-associated cancers tend to arise within mucosa affected by colonic inflammation (2,3), with precursors recognized as low- to high-grade dysplasias that may spread over large areas (2,4). Although morphological characteristics during remodeling of regenerated colorectal mucosa of IBD patients have been well documented (5–7), molecular events in early processes of carcinogenesis before development of dysplasia have yet to be clearly defined and how chronic inflammation actually contributes to tumor development remains to be clarified (8).

Abbreviations: DMH, 1,2-dimethylhydrazine; DSS, dextran sodium sulfate; IBD, inflammatory bowel disease; PCR, polymerase chain reaction; UC, ulcerative colitis.

Somatic mutations of tumor suppressor *adenomatous polyposis coli* (*APC*) genes, which are known to play crucial roles in sporadic colorectal carcinogenesis (9,10), and APC-associated *β-catenin* mutations, frequently detected in colorectal tumors lacking *APC* mutations (11,12), have been demonstrated to be rare in UC-related tumors (13). Hypermethylation of the *APC* gene has also been shown in sporadic colorectal carcinomas (14), but this has not yet been demonstrated in Crohn's disease or UC-related lesions. On the other hand, assessment of allele loss at microsatellite markers close to known or putative tumor suppressor genes and immunohistochemical analysis in UC-associated dysplasias and carcinomas revealed moderate to high frequencies of allele loss near *APC* (31%, $n = 48$) or *β-catenin* (27%, $n = 55$) genes and altered expression of APC and β-catenin proteins in both UC-related and sporadic tumors (15,16), suggesting that some alterations in the genes associated with the APC/β-catenin/Tcf signal transduction pathway might occur in UC-related carcinogenesis.

To establish experimental models relevant to colitis-associated neoplasia in humans, oral administration of dextran sodium sulfate (DSS), a synthetic sulfated polysaccharide composed of dextran with sulfated anhydroglucose units, to mice, rats or hamsters, with or without pretreatment of colon carcinogens, has been widely utilized (17–23). Since DSS is assumed to be non-genotoxic (24,25) but reported to induce erosion, ulceration and/or inflammation of colorectal mucosa in mice and rats (19,25,26), its effects are at least partly due to tumor promotion as a result of regenerative proliferation. However, a 7 day DSS treatment was shown to be sufficient to induce dysplasias after a 180 day withdrawal period in mice (27), so that irreversible molecular events may also occur in association with DSS-induced mucosal damage and/or inflammation. Information concerned with mechanisms underlying DSS-induced colorectal carcinogenesis has recently accumulated from studies of mouse models (28–30).

In rat, colon carcinogenesis induced by genotoxic carcinogens, several morphological and molecular events in early stages have also been well documented. As putative pre-neoplastic lesions, aberrant crypt foci (31), β-catenin accumulated crypts (32), mucin-depleted foci (33), dysplastic aberrant crypt foci (34) and flat dysplastic aberrant crypt foci (35) have been proposed. As a genetic alteration, mutation of *β-catenin* in such pre-neoplastic lesions is reported to be an early event (34,36–38). On the other hand, morphological and molecular investigations of colitis-induced rat models have been limited. Recently, we have established a rapid carcinogenesis model in rats initiated with 1,2-dimethylhydrazine (DMH) followed by a 1 week DSS treatment, in which neoplastic lesions including adenocarcinomas localized in distal parts of the colon/rectum can be induced within 10 weeks (39). This model has been utilized for detection of colorectal carcinogenesis modifiers, applying neoplastic lesions as end-points, within a short-term period (40), but possible mechanisms of the DSS-induced colitis-associated tumor promotion have yet to be explored in detail. With respect to roles of the APC/β-catenin pathway in DSS-associated carcinogenesis, immunohistochemistry for β-catenin revealed an altered subcellular localization in neoplasms in some mouse models treated with DSS with or without carcinogen pretreatment (28,29), but early events in the colorectal mucosa are not completely understood. In the present study, to characterize the early morphological characteristics and genetic events of colorectal mucosa in the DMH–DSS rat model, time-course histopathological analyses, with immunohistochemistry for β-catenin and genetic analysis for *β-catenin*, were performed. In addition, cell proliferation kinetics in the reactive hyperplastic/regenerative mucosa after DSS-induced damage were analyzed with reference to expression of β-catenin, known to regulate epithelial cell growth (41,42).

Materials and methods

Chemicals and animals

DMH was purchased from Tokyo Kasei Kogyo (Tokyo, Japan) and DSS (Molecular weight 36 000–50 000) was from ICN Biochemicals (Aurora, OH). A total of 28 male F344 rats at 6 weeks of age were purchased from Japan SLC (Shizuoka, Japan) and housed four rats per polycarbonate cage with white wood chips (Sankyo Laboratory Service, Tokyo, Japan) for bedding in a standard air-conditioned room (24 ± 1°C, 55 ± 5% relative humidity, 12 h light and dark cycle), with free access to basal diet (CRF-1; Oriental Yeast, Tokyo, Japan) and tap water.

Experimental protocol

Twenty of 28 animals were given three subcutaneous injections of DMH (40 mg/kg body wt, dissolved at 8 mg/ml in saline) in the first week and allowed free access to deionized water containing 1% DSS for 1 week thereafter, as described earlier (40). These animals were then given basal diet and tap water *ad libitum*. At weeks 1, 4, 6 and 8 after DSS treatment, 4, 8, 4 and 4 rats, respectively, were euthanized by exsanguination under deep ether anesthesia for collection of colorectal samples. The remaining eight non-initiated animals were maintained without DMH or DSS treatment and four animals each were euthanized at weeks 1 and 4 for control sample collection. At autopsy, the entire colon and rectum of each animal were excised, opened longitudinally, stretched flat with needles on styrofoam board and fixed in 10% neutral buffered formalin.

Histopathological observations

The fixed entire colons and rectums of four DMH–DSS-treated animals at each time point and control animals at week 1 were cut into three equal lengths from the proximal to the distal ends, and the distal part was additionally cut longitudinally into two strips and routinely embedded in paraffin. Serial sections were prepared for staining with hematoxylin and eosin, immunohistochemistry and/or DNA extraction. The middle and proximal colon were cut longitudinally into two strips and similarly processed to hematoxylin and eosin stained sections. Proportions of regenerative mucosa with or without Paneth cell metaplasia in total mucosal (muscularis musosae) length of the sectioned distal colon and rectum of each animal and proportions of regions accompanied by interstitial inflammation in the regenerative mucosa with or without Paneth cell metaplasia were measured with an IPAP-WIN morphometric analyzer (Sumika Technoservice, Hyogo, Japan). The fixed distal part of the remaining four DMH–DSS-treated and control animals each at week 4 was processed into serial paraffin sections of the middle to lower crypt zone of mucosa by *en face* preparation (36) and stained with hematoxylin and eosin and immunohistochemistry, to investigate architectural characteristics of regenerative mucosa and location of pre-neoplastic lesions in large mucosal areas. Pre-neoplastic and neoplastic lesions of colorectal mucosa were histopathologically classified into dysplastic foci, adenomas and adenocarcinomas as described earlier in rat colorectal carcinogenesis models (20,25,34).

Immunohistochemistry

Monoclonal antibody against β-catenin was purchased from BD Transduction Laboratories (clone 14, Lexington, KY) used at a dilution of 1/500 and an anti-rat Ki-67 antigen for determination of cell proliferative activities from DAKO (clone MIB-5, Glostrup, Denmark) used at 1/100. Antigen retrieval was performed in an autoclave for 15 min at 121°C in 10 mM citrate buffer (pH 6.0) for both β-catenin and Ki-67. The streptavidin–biotin peroxidase complex method (StreptABComplex/HRP, DAKO) or a peroxidase-labeled amino acid polymer method (Histofine simple stain rat MAX-PO, Nichirei Bioscience, Tokyo, Japan) was used to determine the expression and localization of each antigen, and sections were lightly counterstained with hematoxylin for microscopic examination. Negative controls were included without primary antibodies for each antigen using serial sections. In the lesions sampled for mutation analysis described below, immunohistochemical intensity for β-catenin was evaluated as weak to moderate, which means ≤50% of crypts contained β-catenin-positive epithelial cells, or strong, which means >50% positive cells in each lesion. Ki-67-positive nuclei per 300–1400 epithelial cells were counted in randomly selected regions of normal-appearing mucosa and reactive hyperplastic mucosa from all DMH–DSS-treated animals at week 1 and of normal-appearing mucosa and regenerative mucosa with and without Paneth cells from DMH–DSS-treated animals at weeks 4 and 6.

Mutation analysis of β-catenin

DNA extraction from paraffin-embedded sections was performed as follows. Lesions were dissected under a microscope using the Pinpoint Slide DNA Isolation System (Zymo Research, Orange, CA) according to the manufacturer's protocol. Extracted DNA was then subjected to polymerase chain reaction (PCR)-based direct sequencing using the CEQ2000XL DNA analysis system (Beckman Coulter, Fullerton, CA). PCR primers for the rat *β-catenin* gene were designed to amplify the 193 bp fragment from exon 3, corresponding to phosphorylation sites. Primer sequences were 5′-TGACCTCATGGAGTTGGACA-3′ for forward, 5′-GCCTTGCTCCCACTCATAAA-3′ for reverse and with an annealing temperature of 60°C. PCR reactions were performed using AmpliTaq Gold DNA polymerase (Applied Biosystems Japan,

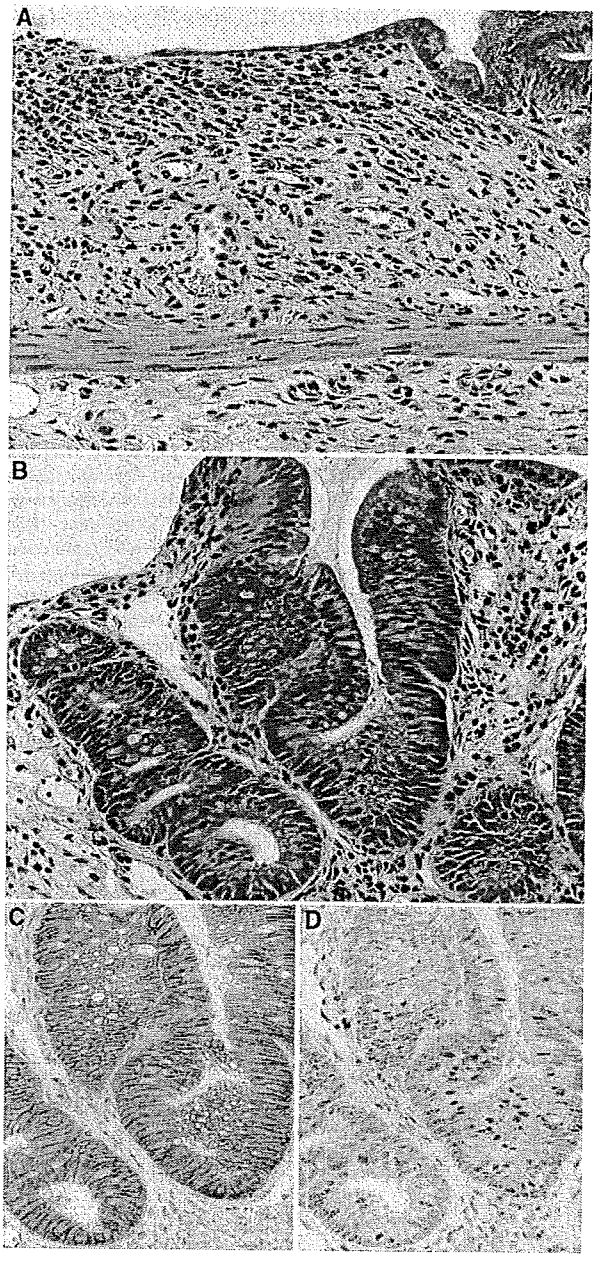

Fig. 1. Colorectal mucosal lesions of rats after week 1 of DSS treatment following DMH initiation. (**A**) Regional erosion accompanied by inflammatory cell infiltration, edema and fibrosis in lamina propria and/or submucosa. Hematoxylin and eosin. Original magnification, ×180. (**B**) Reactive mucosal hyperplasia featuring an irregular glandular structure without distinct cellular atypia. Hematoxylin and eosin. Original magnification, ×180. (**C**) A serial section of (**B**). Note immunoreactivity of β-catenin in the epithelial cells. β-catenin—immunohistochemistry. (**D**) A serial section of (**B**). Distinct Ki-67 positivity is shown in the reactive hyperplastic epithelial cells. Ki-67—immunohistochemistry.

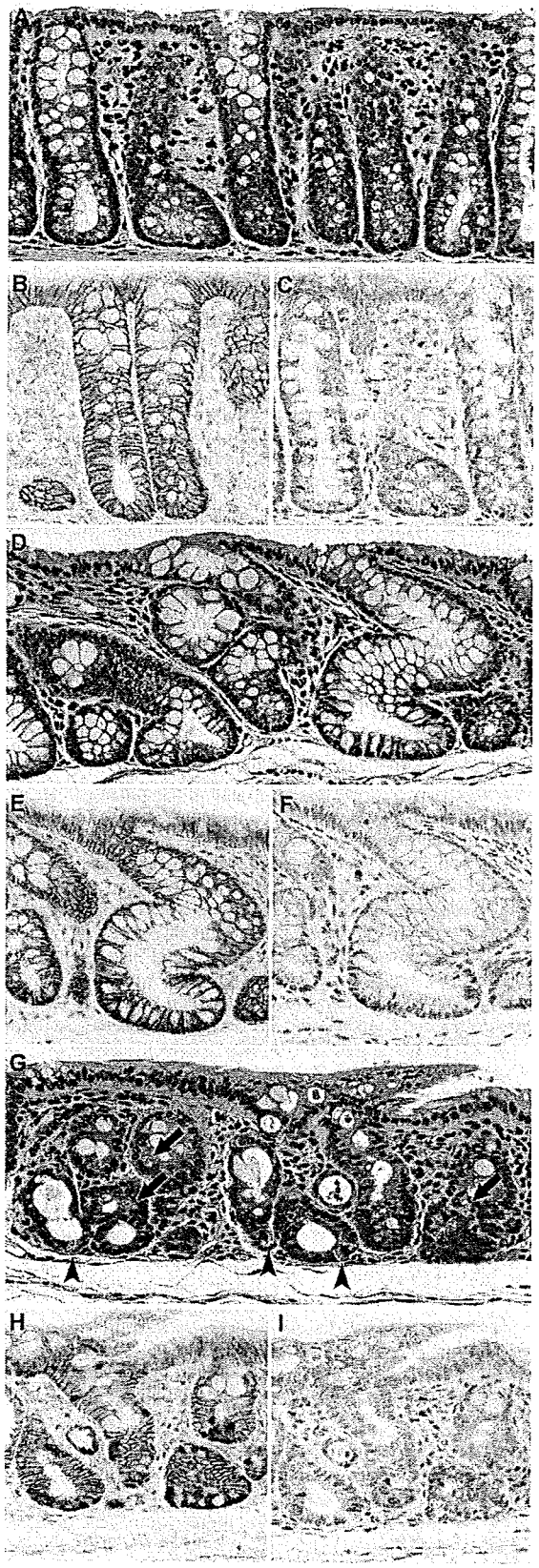

Tokyo, Japan). Nested sequence primers used for direct sequencing of the PCR products were 5′-CAGACAGAAAGGCCGCTGT-3′ and 5′-CATCTTCTTCCTCAGGATTGC-3′ for forward and reverse, respectively. Mutation analyses were performed twice for forward and once for reverse to confirm the results.

Statistical analysis

Statistical analysis to compare the proportions of regenerative mucosa with or without Paneth cell metaplasia, the proportions of regions accompanied by interstitial inflammation in the regenerative mucosa with or without Paneth cell metaplasia and the Ki-67 labeling indices was performed with the Student's or Welch's *t*-test following the *F* test. Significance was inferred at the 5%, 1% and 0.1% levels.

Results

General conditions and body weight

After 1 week of DSS treatment, a few rats showed bloody/soft stools. Thereafter, no such clinical symptoms were observed. Body weight gain of DMH–DSS-treated animals was significantly ($P < 0.05$) smaller than the no-treatment controls (initial body weights and values week 1 after DSS treatment were 135.4 ± 5.5 and 197.4 ± 14.7 g, respectively, for DMH–DSS-treated rats and 135.6 ± 4.1 and 218.2 ± 5.6 g for control rats).

Gross findings and histopathology

At necropsy, after 1 week of DSS treatment, no obvious macroscopic changes were detected, except for slight roughening of the surface in the distal parts of the colon and rectal mucosa of DMH–DSS-treated animals. At weeks 6 and 8, polypoid/protruded nodules were observed in the distal part of the colon and rectal mucosa of 2 of 4 animals each. In a total of three animals without nodules, a cloudy area of mucosal surface continuous from anus to rectum/distal colon, corresponding to histopathological squamous metaplasia described below, was visible at weeks 4 and 6. Also, on microscopic observation, major changes were observed in the distal colon and rectum. At week 1, regional loss of crypts, so-called erosion, accompanied by severe inflammatory cell infiltration, consisting mainly of neutrophils and foamy mononuclear cells, and various degrees of edema and fibrosis in the lamina propria and/or submucosa, was noted in all DMH–DSS-treated animals (Figure 1A). Reactive mucosal hyperplasia accompanied by mucosal thickening in areas neighboring erosion was also frequently detected in all animals. Some crypts in the reactive hyperplastic mucosa were simply elongated and lined by hyperplastic epithelium with goblet cells, while some featured an irregular glandular structure lined by hyperplastic basophilic epithelium with neither goblet cells nor distinct cellular atypia (Figure 1B). Others were intermediate in appearance. At weeks 4–8, mucosal damage and pronounced inflammatory

Fig. 2. Colorectal mucosal lesions at week 4–6 in routinely longitudinally embedded sections after DSS treatment following DMH initiation. (**A**) Normal mucosa of a non-treated control rat. Hematoxylin and eosin. Original magnification, ×180. (**B**) A serial section of (**A**). Note immunoreactivity of β-catenin in the epithelial cells. β-catenin—immunohistochemistry. (**C**) A serial section of (**A**). Note Ki-67-positive cells in the lower crypt zone. Ki-67—immunohistochemistry. (**D**) Regenerative mucosa showing distortion and/or dilatation of crypts without distinct cellular atypia. Hematoxylin and eosin. Original magnification, ×180. (**E**) A serial section of (**D**). Note immunoreactivity of β-catenin in the epithelial cells. β-catenin—immunohistochemistry. (**F**) A serial section of (**D**). Note Ki-67-positive cells in the lower crypt zone. Ki-67—immunohistochemistry. (**G**) Regenerative mucosa with Paneth cell metaplasia, characterized by cytoplasmic eosinophilic granules, in the lower crypt zone (arrowheads) and middle zone (arrows). Crypts show distortion and shortening. Hematoxylin and eosin. Original magnification, ×180. (**H**) A serial section of (**G**). Nuclear/cytoplasmic expression of β-catenin in subsets of epithelial cells. β-catenin—immunohistochemistry. (**I**) A serial section of (**G**). Note Ki-67-positive cells in the lower crypt zone and the middle zone. Ki-67—immunohistochemistry.

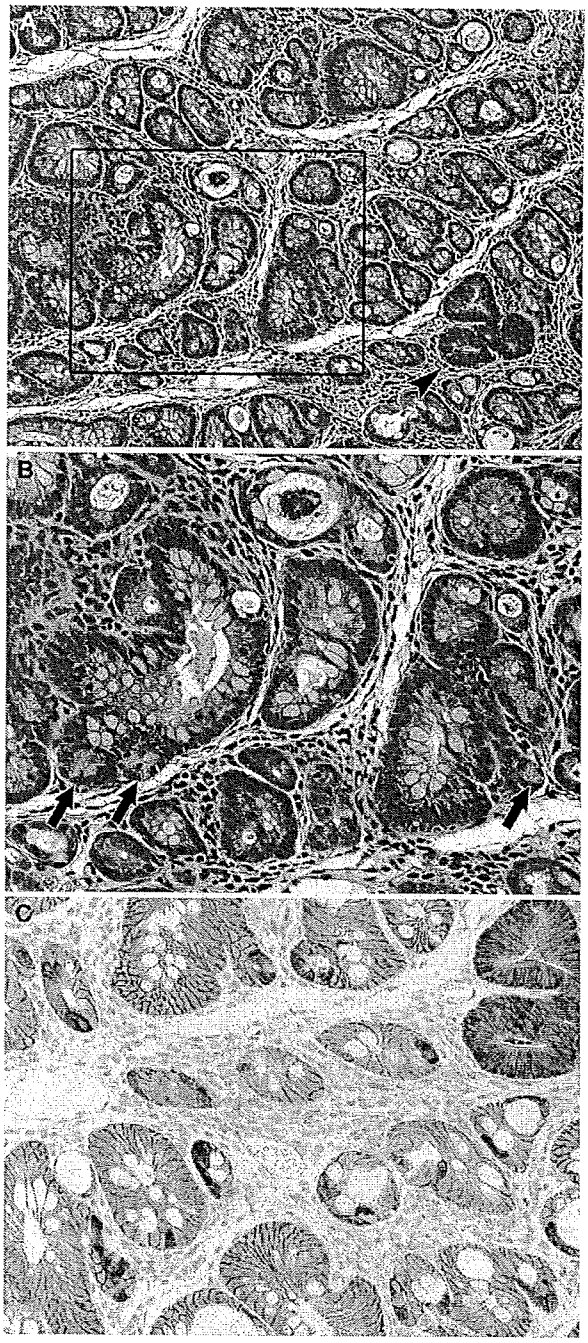

Fig. 3. Colorectal mucosal lesions in sections after *en face* preparation at week 4 after DSS treatment following DMH initiation. (**A**) Regenerative mucosa with interstitial inflammation and Paneth cell metaplasia. A dysplastic focus (arrowhead) is also included. Hematoxylin and eosin, ×90. (**B**) A higher magnification of the box in (**A**). Paneth cells frequently observed in laterally branching crypts (arrows), ×180. (**C**) A serial section of (**A**). Note nuclear/cytoplasmic expression of β-catenin in the dysplastic focus and subsets of epithelial cells in the regenerative mucosa with Paneth cells. β-catenin—immunohistochemistry, ×180.

cell infiltration were no longer evident. Instead, regenerative mucosa showing abnormal cryptal architecture, with distortion, dilatation, branching and/or shortening of crypts, with or without mucosal atrophy and variation in inter-crypt spacing, was observed (Figures 2A, D and G and 3A). The regenerative mucosa was characterized by minimal cellular atypia and goblet cell differentiation. Especially in some regions with interstitial inflammatory cell infiltration, Paneth cell metaplasia characterized by cytoplasmic eosinophilic granules was frequently seen (Figure 2G and 3A). Data for proportions of regenerative mucosa with or without Paneth cell metaplasia in longitudinally embedded sections at each time point are summarized in Table I. The values regenerative mucosa with Paneth cells peaked at week 4, with tendencies to decrease thereafter. Regenerative mucosa with Paneth cells was significantly ($P < 0.01$) more associated with interstitial inflammation than regenerative mucosa without Paneth cells (Table I). The Paneth cells appeared mainly in the lower crypt zone but also in the middle zone in the longitudinally embedded sections (Figure 2G), and in the sections by an *en face* preparation they were frequently observed in laterally branching crypts in the middle zone (Figure 3B). Dysplastic foci, accompanied by moderate cellular atypia and almost lacking goblet cells, arose at weeks 4–8 and adenomas and adenocarcinomas at weeks 6 and 8 (Table II). Eight of 11 (73%) dysplastic foci found in the routinely longitudinally embedded sections on weeks 4–8 and nine of 13 (69%) dysplastic foci found in the sections by an *en face* preparation on week 4 were surrounded by regenerative mucosa with Paneth cells (Figures 3A). Eleven of 24 (46%) dysplastic foci, three of 4 adenomas and one adenocarcinoma featured various degrees of Paneth cell differentiation. The macroscopic cloudy mucosal surface observed on weeks 4 and 6 was confirmed as squamous metaplasia of the colorectal mucosa, continuous from the anus. Microscopic findings in the middle and proximal colon were limited to diffuse mucosal thickening and increased size of mucosal lymphoid follicles at weeks 1–6 and weeks 1–8, respectively.

Immunohistochemistry and cell proliferative activity

Immunoreactivity of β-catenin was found in the epithelial cells (Figure 2B) with weak reactions in the endothelium of blood vessels and ganglion cells in submucosal and myenteric (Meissner's and Auerbach's) plexus in non-treated control rats. No obvious aberrant expression of β-catenin in mucosal epithelium was detected at week 1 in DMH–DSS-treated animals (Figure 1C). At weeks 4–8, nuclear/cytoplasmic expression of β-catenin was exhibited in subsets of epithelial cells in the regenerative mucosa with Paneth cell metaplasia (Figure 2H and 3C) but this was not evident in tissue without Paneth cells (Figure 2E). The β-catenin-accumulated epithelial cells with and without Paneth cell metaplasia were frequently located not only in the lower crypt zone (Figure 2H) but also in laterally branching crypts in the middle zone (Figure 3C). Accumulation of β-catenin was also detected in the dysplastic foci, adenomas and adenocarcinomas, with higher levels of expression than in the regenerative mucosa with Paneth cells (Figure 3C). Ki-67 positivity of epithelial cells in the reactive hyperplastic mucosa was significantly ($P < 0.01$) greater than that in normal mucosa in the controls and normal-appearing mucosa in the DMH–DSS-treated animals at week 1 (Figure 1D and 2C, Table III), whereas values for regenerative mucosa with and without Paneth cell metaplasia and β-catenin accumulation were similar, and significantly ($P < 0.05$) lower than in normal-appearing mucosa at weeks 4–6 (Figure 2F and I, Table III). Ki-67-positive cells were mainly localized in the lower crypt zone of the regenerative mucosa without Paneth cell metaplasia, but with Paneth cell metaplasia the Ki-67-positive cells were detected not only in the lower zone but also in the middle zone of the regenerative mucosa.

Mutations of the β-catenin gene in regenerative and neoplastic lesions

Twenty-seven regenerative lesions with Paneth cell metaplasia, five dysplastic foci with Paneth cells, one dysplastic focus without Paneth cells, two adenomas and one adenocarcinoma with Paneth cells could be subjected to PCR-based direct sequencing for the *β-catenin* gene. Six of 27 (22%) regenerative and two of six (33%) dysplastic foci and one adenoma and carcinoma each were found to harbor point

Table I. Proportions of regenerative mucosa with or without Paneth cell metaplasia in the distal colon and rectal mucosa of rats treated with DSS after DMH initiation

Week after DSS administration	No. of rats analyzed	Regenerative mucosa					
		With Paneth cell metaplasia			Without Paneth cell metaplasia		
		Incidence	% of total mucosal length	% of length accompanied by interstital inflammation	Incidence	% of total mucosal length	% of length accompanied by interstital inflammation
1	4	0	—	—	0	—	—
4	4	4	17.9 ± 8.1	42.2 ± 14.1[a]	4	32.5 ± 8.4	8.7 ± 5.6
6	4	4	8.8 ± 7.8	38.3 ± 26.6	4	32.4 ± 11.3	18.2 ± 21.5
8	4	2	5.6 ± 10.3	13.8 ± 27.6	3	13.7 ± 10.3	4.5 ± 9.0
Control	4	—			—		

Mean ± SD.
The values are based on the findings with longitudinally embedded sections.
[a]$P < 0.01$ versus regenerative mucosa without Paneth cell metaplasia (Student's t-test).

Table II. Incidences and numbers of pre-neoplastic and neoplastic lesions in the distal colon and rectal mucosa of rats treated with DSS after DMH initiation

Week after DSS administration	No. of rats analyzed	Dysplastic foci		Adenoma		Adenocarcinoma	
		Incidence	Number/rat	Incidence	Number/rat	Incidence	Number/rat
1	4	0	—	0	—	0	—
4	4	1	0.3 ± 0.1	0	—	0	—
6	4	3	1.8 ± 1.7	1	0.3 ± 0.1	1	0.3 ± 0.1
8	4	2	0.8 ± 1.0	2	0.8 ± 1.0	0	—
Control	4	—		—		—	

Mean ± SD.
The values are based on findings with longitudinally embedded sections.

Table III. Cell proliferative activity in reactive hyperplastic mucosa and regenerative mucosa in the distal colon/rectum of rats treated with DSS after DMH initiation

Week after DSS administration	Type of lesion[a]	No. of rats analyzed	Ki-67 positivity[b] (%)
1	Normal-appearing mucosa	4	38.7 ± 12.4
	Reactive hyperplastic mucosa	4	73.2 ± 12.7[c]
4–6	Normal-appearing mucosa	8	34.4 ± 9.3
	RM with Paneth cell metaplasia/β-catenin accumulation	8	25.9 ± 8.4[d]
	RM without Paneth cell metaplasia/β-catenin accumulation	7	23.3 ± 7.3[d]
Control	Normal mucosa	4	38.9 ± 12.6

[a]RM, regenerative mucosa.
[b]Mean ± SD.
[c]$P < 0.01$.
[d]$P < 0.05$ versus corresponding normal-appearing mucosa.
The values are based on findings with longitudinally embedded sections.

mutations. Data for mutation status for phosphorylation sites and mutation hot spots of *β-catenin* gene are summarized in Table IV. Mutations at codons 34 and 41 were the most common, and all mutations found in the lesions caused amino acid substitution. No significant correlation between the mutation status and immunohistochemical intensity for β-catenin was observed across lesions.

Discussion

In the present study, distal parts of the colon and rectal mucosa were found to undergo extensive loss of crypts along with inflammatory cell infiltration and neighboring reactive hyperplasia in rats after 1 week DSS treatment following DMH initiation. Repair was evident within several weeks with the appearance of regenerative mucosa having an abnormal architecture but lacking distinct cellular atypia. In the regenerative mucosa, particularly in regions with inflammatory change, Paneth cell metaplasia was additionally characterized. In quiescent phase or long-standing cases of IBD patients, similar histopathological changes including crypt distortion, mucosal atrophy and Paneth cell metaplasia have been described (7). In addition, Paneth cell metaplasia is particularly numerous in patients with long-standing colitis who develop malignant change (7), although the underlying etiology of the Paneth cell metaplasia in response to injury has yet to be clarified (43). Whether the re-epithelialization of large patches of colonic mucosa by abnormal clones is simply a consequence of the healing response to ulceration caused by chronic inflammation or the epithelial cells of IBD patients have an innate ability to replace surrounding epithelium is also unknown (2). Both DMH-induced tumors and DSS-induced mucosal damaged/reactive changes are more prevalent in the distal part of the colon/rectum in rats (44,45), suggesting promoting effects of DSS-associated mucosal lesions on DMH-induced carcinogenesis to be limited to the affected tissue. In our previous experiment, Paneth cell metaplasia in non-dysplastic/neoplastic colorectal mucosa did not appear in rats treated with DMH or DSS alone (39). Therefore, the cause of Paneth cell metaplasia induced within several weeks after DSS treatment in the present rat model, in contrast to long-standing IBD cases, remains unknown, but DMH initiation is presumably associated with the differentiation abnormality

Table IV. Mutation status of the β-*catenin* in regenerative mucosa samples with Paneth cell metaplasia and pre-neoplastic and neoplastic lesions in the distal colon and rectal mucosa of rats treated with DSS after DMH initiation

Sample	Week after DSS administration	Immunohistochemical intensity for β-catenin[a]	Mutation status		
			Codon	Type of mutation	AA substitution
RM	4	+	34	GGA→GAA	Gly→Glu
RM	4	+	34	GGA→GAA	Gly→Glu
RM	4	++		Wild type	
RM	4	++		Wild type	
RM	4	+		Wild type	
RM	4	+		Wild type	
RM	4	+		Wild type	
RM	4	+		Wild type	
RM	4	+		Wild type	
RM	6	++	33	TCT→TGT	Ser→Cys
RM	6	+	34	GGA→GAA	Gly→Glu
RM	6	+	41	ACC→ATC	Thr→Ile
RM	6	++		Wild type	
RM	6	++		Wild type	
RM	6	++		Wild type	
RM	6	++		Wild type	
RM	6	+		Wild type	
RM	6	+		Wild type	
RM	6	+		Wild type	
RM	6	+		Wild type	
RM	6	+		Wild type	
RM	6	+		Wild type	
RM	6	+		Wild type	
RM	6	+		Wild type	
RM	8	+	41	ACC→ATC	Thr→Ile
RM	8	++		Wild type	
RM	8	++		Wild type	
Dy	4	+		Wild type	
Dy	6	+	34	GGA→GAA	Gly→Glu
Dy[b]	6	+	41	ACC→ATC	Thr→Ile
Dy	6	++		Wild type	
Dy	8	++		Wild type	
Dy	8	++		Wild type	
Ad	8	++	41	ACC→ATC	Thr→Ile
Ad	8	++		Wild type	
Ca	6	++	37	TCT→TTT	Ser→Ile

RM, regenerative mucosa with Paneth cell metaplasia; Dy, dysplastic focus; Ad, adenoma; Ca, adenocarcinoma.
[a]+, weak to moderate; ++, strong.
[b]Dysplasia without Paneth cell metaplasia.

which is only likely to occur in rats treated with DMH and DSS. Most dysplastic foci were found in regions with Paneth cells, and the fact that dysplastic and neoplastic lesions also frequently showed Paneth cell differentiation suggests that substantial genomic alterations associated with DSS-induced mucosal damage can occur and contribute to carcinogenesis.

A striking feature in the present study was the alteration in subcellular localization of β-catenin exhibited by subsets of epithelial cells in the regenerative mucosa with Paneth cells. Point mutations of *β-catenin* gene were also detected in 6 of 27 regenerative mucosa samples with Paneth cells. Thus, accumulation of β-catenin might have been caused, at least partly, by gene alterations occurring in the regenerative colorectal mucosa with Paneth cells in the DMH–DSS rats. In our previous experiment, β-catenin accumulation in non-dysplastic/neoplastic colorectal mucosal lesions was not evident in rats treated with DMH or DSS alone (39). Although *β-catenin* mutations have previously been found in early dysplastic lesions in rat colorectal carcinogenesis induced by genotoxic carcinogens (34,36,44), to our knowledge, this is the first report of their demonstration in non-dysplastic tissue after mucosal damage in rodent colorectal carcinogenesis. In previous literature, *β-catenin* gene mutations, most commonly at codon 32, were demonstrated in early dysplastic lesions and tumors induced by DMH (44), and another report showed the mutation cluster around codon 33 in DMH-induced tumors in the rat colon (46). With the non-dysplastic regenerated mucosa with Paneth cells, dysplastic foci and tumors analyzed in the present study, *β-catenin* mutations at codons 34 and 41 were the most common. Interestingly, the mutated codon 41 directly substitutes a critical threonine phosphorylation site (47) and has been found in human colon tumors with wild-type *APC* (11). Yamada *et al.* have demonstrated *β-catenin* mutations to be scattered in exon 3 of the gene in early dysplastic lesions, while they are converged at codons encoding functionally important residues in tumors in azoxymethane-induced rat colon carcinogenesis. This indicates *β-catenin* mutations to be selected during malignant transformation (48). On the other hand, Blum *et al.* showed that the spectrum of *β-catenin* mutations in carcinogen-induced rat colon tumors can be altered from a cluster around Ser33 to codons 37, 41 and 45 by post-initiation exposure to a phytochemicals. Thus, we can speculate the existence of a survival advantage for cells containing mutant forms of *β-catenin* with substitutions in Ser37, Thr41 or Ser45 (46). The present results are clearly in line with DSS-associated mucosal damage causing cell proliferation in reactive hyperplastic mucosa and acceleration of such mutated gene selection to promote rat colorectal carcinogenesis.

Neoplastic transformation and progression are known to be associated with the release of highly reactive oxygen and nitrogen species and/or cytokines from inflammatory cells (2,49) and the regenerative mucosa with Paneth cells was significantly linked to interstitial

inflammation in the present study. Therefore, inflammatory changes not only in the early mucosal damaged condition but also in the subsequent duration with mucosal repair and regeneration under Paneth cell inducing conditions might also play roles. The cause of the decreased proportion of regenerative mucosa with Paneth cells and β-catenin accumulation at later time points, suggesting the aberrant phenotype in regenerative mucosa to be partly reversible, is unclear. Although subsets of β-catenin-accumulated epithelial cells might have pre-neoplastic potential, there is possibility that other more 'normal' subsets are easily affected by cytotoxic inflammatory cells.

No significant correlation between the mutation status and immunohistochemical intensity for β-catenin in the lesions was observed, suggesting *β-catenin* mutations might not be sufficient in themselves for accumulation of the protein. A similar phenomenon has been demonstrated in pre-neoplastic and neoplastic lesions in the colons of carcinogen-treated rats (36,46). Further study is needed to clarify the existence of alterations in other related factors within the APC/β-catenin/Tcf signal transduction pathway. β-Catenin regulates expression of growth-promoting proteins, such as c-myc (41) and cyclin D1 (42), and increased β-catenin expression is accompanied by nuclear translocation in murine colon epithelium (50). Therefore, the accumulation of β-catenin in the regenerative mucosa with Paneth cells might indicate dysfunction of cell proliferation regulatory signals and potential oncogenesis. Wnt signaling, which is transduced through β-catenin/Tcf-4 in intestinal crypts, has recently been reported to drive a Paneth cell maturation program (51). In addition, Andreu *et al.* (52) demonstrated that activation of the β-catenin signaling pathway following *APC* loss promoted differentiation along the Paneth cell lineage in small intestinal epithelial cells in a transgenic mouse model. Accumulation of β-catenin associated with gene mutations might therefore be causally linked with the Paneth cell differentiation of the epithelial cells in the regenerative mucosa and neoplastic lesions in the present rat model. This conclusion is not necessarily inconsistent with the presence of one dysplastic focus without Paneth cell metaplasia containing a mutation at codon 41, since enhanced β-catenin signaling does not appear to be sufficient for the complete differentiation of Paneth cells, as identified by the presence of typical secretory granules (53,54).

In conclusion, regenerative mucosa with Paneth cells, β-catenin accumulation and interstitial inflammatory cell infiltration is possibly involved in the acceleration of colorectal carcinogenesis in this DMH–DSS rat model. The model resembles human IBD cases regarding inflammation-associated Paneth cell metaplasia, but β-catenin accumulation is not necessarily consistent with the human situation. Epithelial regeneration accompanied by chronic inflammation, thus, might induce non-genetic alteration as well as gene mutations and mutated gene selection as a part of the oncogenic events in both humans and experimental animals.

Funding

The Grant-in-Aid for Cancer Research (17S-6) from the Ministry of Health, Labour and Welfare of Japan.

Acknowledgements

We thank Ms Ayako Kaneko for her expert technical assistance.

Conflict of Interest statement: None declared.

References

1. Greenstein,A.J. (2000) Cancer in inflammatory bowel disease. *Mt. Sinai J. Med.*, **67**, 227–240.
2. Itzkowitz,S.H. *et al.* (2004) Inflammation and cancer IV. Colorectal cancer in inflammatory bowel disease: the role of inflammation. *Am. J. Physiol. Gastrointest. Liver Physiol.*, **287**, G7–G17.
3. Rutter,M.D. *et al.* (2004) Cancer surveillance in longstanding ulcerative colitis: endoscopic appearances help predict cancer risk. *Gut*, **53**, 1813–1816.
4. Sigel,J.E. *et al.* (1999) Intestinal adenocarcinoma in Crohn's disease: a report of 30 cases with a focus on coexisting dysplasia. *Am. J. Surg. Pathol.*, **23**, 651–655.
5. Fujii,S. *et al.* (2002) Ulcerative colitis-associated neoplasia. *Pathol. Int.*, **52**, 195–203.
6. Mitsuhashi,J. *et al.* (2005) Significant correlation of morphological remodeling in ulcerative colitis with disease duration and between elevated p53 and p21 expression in rectal mucosa and neoplastic development. *Pathol. Int.*, **55**, 113–121.
7. Day,D.W. *et al.* (2003) Inflammatory disorders of the large intestine. In Marson and Dawson (eds.) *Gatrointestinal Pathology, Fourth Edition.* Blackwell Science, Oxford, pp. 472–539.
8. Baisse,B. *et al.* (2004) Synchronous ileal and colonic adenocarcinomas associated with Crohn's disease: report of a case with a focus on genetic alterations and carcinogenesis. *J. Clin. Pathol.*, **57**, 885–887.
9. Powell,S.M. *et al.* (1992) APC mutations occur early during colorectal tumorigenesis. *Nature*, **359**, 235–237.
10. Miyoshi,Y. *et al.* (1992) Somatic mutations of the APC gene in colorectal tumors: mutation cluster region in the APC gene. *Hum. Mol. Genet.*, **1**, 229–233.
11. Sparks,A.B. *et al.* (1998) Mutational analysis of the APC/beta-catenin/Tcf pathway in colorectal cancer. *Cancer Res.*, **58**, 1130–1134.
12. Mirabelli-Primdahl,L. *et al.* (1999) Beta-catenin mutations are specific for colorectal carcinomas with microsatellite instability but occur in endometrial carcinomas irrespective of mutator pathway. *Cancer Res.*, **59**, 3346–3351.
13. Aust,D.E. *et al.* (2002) The APC/beta-catenin pathway in ulcerative colitis-related colorectal carcinomas: a mutational analysis. *Cancer*, **94**, 1421–1427.
14. Esteller,M. *et al.* (2000) Analysis of adenomatous polyposis coli promoter hypermethylation in human cancer. *Cancer Res.*, **60**, 4366–4371.
15. Tomlinson,I. *et al.* (1998) A comparison of the genetic pathways involved in the pathogenesis of three types of colorectal cancer. *J. Pathol.*, **184**, 148–152.
16. Aust,D.E. *et al.* (2001) Altered distribution of beta-catenin, and its binding proteins E-cadherin and APC, in ulcerative colitis-related colorectal cancers. *Mod. Pathol.*, **14**, 29–39.
17. Okayasu,I. *et al.* (1996) Promotion of colorectal neoplasia in experimental murine ulcerative colitis. *Gut*, **39**, 87–92.
18. Okayasu,I. *et al.* (2002) Dysplasia and carcinoma development in a repeated dextran sulfate sodium-induced colitis model. *J. Gastroenterol. Hepatol.*, **17**, 1078–1083.
19. Hirono,I. *et al.* (1981) Induction of intestinal tumors in rats by dextran sulfate sodium. *J. Natl Cancer Inst.*, **66**, 579–583.
20. Hirono,I. *et al.* (1983) Enhancing effect of dextran sulfate sodium on colorectal carcinogenesis by 1,2-dimethylhydrazine in rats. *Gann*, **74**, 493–496.
21. Yamada,M. *et al.* (1992) Occurrence of dysplasia and adenocarcinoma after experimental chronic ulcerative colitis in hamsters induced by dextran sulphate sodium. *Gut*, **33**, 1521–1527.
22. Tanaka,T. *et al.* (2003) A novel inflammation-related mouse colon carcinogenesis model induced by azoxymethane and dextran sodium sulfate. *Cancer Sci.*, **94**, 965–973.
23. Nishikawa,A. *et al.* (2005) Induction of colon tumors in C57BL/6J mice fed MeIQx, IQ, or PhIP followed by dextran sulfate sodium treatment. *Toxicol. Sci.*, **84**, 243–248.
24. Mori,H. *et al.* (1984) Absence of genotoxicity of the carcinogenic sulfated polysaccharides carrageenan and dextran sulfate in mammalian DNA repair and bacterial mutagenicity assays. *Nutr. Cancer*, **6**, 92–97.
25. Whiteley,L.O. *et al.* (1996) Aberrant crypt foci in the colonic mucosa of rats treated with a genotoxic and nongenotoxic colon carcinogen. *Toxicol. Pathol.*, **24**, 681–689.
26. Cooper,H.S. *et al.* (1993) Clinicopathologic study of dextran sulfate sodium experimental murine colitis. *Lab. Invest.*, **69**, 238–249.
27. Cooper,H.S. *et al.* (2000) Dysplasia and cancer in the dextran sulfate sodium mouse colitis model. Relevance to colitis-associated neoplasia in the human: a study of histopathology, beta-catenin and p53 expression and the role of inflammation. *Carcinogenesis*, **21**, 757–768.
28. Fujii,S. *et al.* (2004) Development of colonic neoplasia in p53 deficient mice with experimental colitis induced by dextran sulphate sodium. *Gut*, **53**, 710–716.
29. Tanaka,T. *et al.* (2005) Colonic adenocarcinomas rapidly induced by the combined treatment with 2-amino-1-methyl-6-phenylimidazo[4,5-b]pyridine and dextran sodium sulfate in male ICR mice possess beta-catenin gene mutations and increases immunoreactivity for beta-catenin, cyclooxygenase-2 and inducible nitric oxide synthase. *Carcinogenesis*, **26**, 229–238.

30. Kohno,H. *et al.* (2005) Beta-Catenin mutations in a mouse model of inflammation-related colon carcinogenesis induced by 1,2-dimethylhydrazine and dextran sodium sulfate. *Cancer Sci.*, **96**, 69–76.
31. Bird,R.P. (1987) Observation and quantification of aberrant crypts in the murine colon treated with a colon carcinogen: preliminary findings. *Cancer Lett.*, **37**, 147–151.
32. Yamada,Y. *et al.* (2001) Sequential analysis of morphological and biological properties of beta-catenin-accumulated crypts, provable premalignant lesions independent of aberrant crypt foci in rat colon carcinogenesis. *Cancer Res.*, **61**, 1874–1878.
33. Caderni,G. *et al.* (2003) Identification of mucin-depleted foci in the unsectioned colon of azoxymethane-treated rats: correlation with carcinogenesis. *Cancer Res.*, **63**, 2388–2392.
34. Ochiai,M. *et al.* (2003) Characterization of dysplastic aberrant crypt foci in the rat colon induced by 2-amino-1-methyl-6-phenylimidazo[4,5-b]pyridine. *Am. J. Pathol.*, **163**, 1607–1614.
35. Paulsen,J.E. *et al.* (2005) Flat dysplastic aberrant crypt foci are related to tumorigenesis in the colon of azoxymethane-treated rat. *Cancer Res.*, **65**, 121–129.
36. Yamada,Y. *et al.* (2000) Frequent beta-catenin gene mutations and accumulations of the protein in the putative preneoplastic lesions lacking macroscopic aberrant crypt foci appearance, in rat colon carcinogenesis. *Cancer Res.*, **60**, 3323–3327.
37. Takahashi,M. *et al.* (2000) Altered expression of beta-catenin, inducible nitric oxide synthase and cyclooxygenase-2 in azoxymethane-induced rat colon carcinogenesis. *Carcinogenesis*, **21**, 1319–1327.
38. Tsukamoto,T. *et al.* (2000) More frequent beta-catenin gene mutations in adenomas than in aberrant crypt foci or adenocarcinomas in the large intestines of 2-amino-1-methyl-6-phenylimidazo[4,5-b]pyridine (PhIP)-treated rats. *Jpn. J. Cancer Res.*, **91**, 792–796.
39. Onose,J. *et al.* (2003) Rapid induction of colorectal tumors in rats initiated with 1,2-dimethylhydrazine followed by dextran sodium sulfate treatment. *Cancer Lett.*, **198**, 145–152.
40. Onose,J. *et al.* (2006) A new medium-term rat colon bioassay applying neoplastic lesions as endpoints for detection of carcinogenesis modifiers-validation with known modifiers. *Cancer Lett.*, **232**, 272–278.
41. He,T.C. *et al.* (1998) Identification of c-MYC as a target of the APC pathway. *Science*, **281**, 1509–1512.
42. Tetsu,O. *et al.* (1999) Beta-catenin regulates expression of cyclin D1 in colon carcinoma cells. *Nature*, **398**, 422–426.
43. Longman,R.J. *et al.* (2000) Is the colonic reparative cell lineage yet to be discovered? *Gut*, **47**, 307–308.
44. Femia,A.P. *et al.* (2005) Mucin-depleted foci have beta-catenin gene mutations, altered expression of its protein, and are dose- and time-dependent in the colon of 1,2-dimethylhydrazine-treated rats. *Int. J. Cancer*, **116**, 9–15.
45. Vetuschi,A. *et al.* (2002) Increased proliferation and apoptosis of colonic epithelial cells in dextran sulfate sodium-induced colitis in rats. *Dig. Dis. Sci.*, **47**, 1447–1457.
46. Blum,C.A. *et al.* (2001) beta-Catenin mutation in rat colon tumors initiated by 1,2-dimethylhydrazine and 2-amino-3-methylimidazo[4,5-f]quinoline, and the effect of post-initiation treatment with chlorophyllin and indole-3-carbinol. *Carcinogenesis*, **22**, 315–320.
47. Aberle,H. *et al.* (1997) beta-Catenin is a target for the ubiquitin-proteasome pathway. *EMBO J.*, **16**, 3797–3804.
48. Yamada,Y. *et al.* (2003) beta-Catenin mutation is selected during malignant transformation in colon carcinogenesis. *Carcinogenesis*, **24**, 91–97.
49. Becker,C. *et al.* (2005) IL-6 signaling promotes tumor growth in colorectal cancer. *Cell Cycle*, **4**, 217–220.
50. Sellin,J.H. *et al.* (2001) Increased beta-catenin expression and nuclear translocation accompany cellular hyperproliferation in vivo. *Cancer Res.*, **61**, 2899–2906.
51. van Es,J.H. *et al.* (2005) Wnt signalling induces maturation of Paneth cells in intestinal crypts. *Nat. Cell Biol.*, **7**, 381–386.
52. Andreu,P. *et al.* (2005) Crypt-restricted proliferation and commitment to the Paneth cell lineage following Apc loss in the mouse intestine. *Development*, **132**, 1443–1451.
53. Crawford,H.C. *et al.* (1999) The metalloproteinase matrilysin is a target of beta-catenin transactivation in intestinal tumors. *Oncogene*, **18**, 2883–2891.
54. Batlle,E. *et al.* (2002) Beta-catenin and TCF mediate cell positioning in the intestinal epithelium by controlling the expression of EphB/ephrinB. *Cell*, **111**, 251–263.

Received January 23, 2007; revised May 6, 2007; accepted May 12, 2007

Oncogene (2007) 26, 6194–6202

www.nature.com/onc

ORIGINAL ARTICLE

Bcl-2 overexpression in PhIP-induced colon tumors: cloning of the rat *Bcl-2* promoter and characterization of a pathway involving β-catenin, c-Myc and E2F1

Q Li[1], WM Dashwood[1], X Zhong[1], H Nakagama[2] and RH Dashwood[1]

[1]*Linus Pauling Institute, Oregon State University, Corvallis, OR, USA and* [2]*National Cancer Center Research Institute, Tokyo, Japan*

β-Catenin/T-cell factor (Tcf) signaling is constitutively active in the majority of human colorectal cancers, and there are accompanying changes in Bcl-2 expression. Similarly, 2-amino-1-methyl-6-phenylimidazo(4,5-b)pyridine (PhIP)-induced colon tumors in the rat have increased β-catenin and elevated Bcl-2. To examine the possible direct transcriptional regulation of rat *Bcl-2* by β-catenin/Tcf, we cloned and characterized the corresponding promoter region and found 70.1% similarity with its human counterpart, *BCL2*. *Bcl-2* promoter activity was increased in response to LiCl and exogenous β-catenin, including oncogenic mutants of β-catenin found in PhIP-induced colon tumors. Protein/DNA arrays identified E2F1, but not β-catenin/Tcf, as interacting most strongly with the rat *Bcl-2* promoter. Exogenous E2F1 increased the promoter activity of rat *Bcl-2*, except in mutants lacking the E2F1 sites. As expected, β-catenin induced its downstream target c-Myc, as well as E2F1 and Bcl-2, and this was blocked by siRNA to c-Myc or E2F1. These findings suggest an indirect pathway for Bcl-2 overexpression in PhIP-induced colon tumors involving β-catenin, c-Myc and E2F1.
Oncogene (2007) **26,** 6194–6202; doi:10.1038/sj.onc.1210438; published online 2 April 2007

Keywords: β-catenin; Bcl-2; c-Myc; E2F1; wnt signaling; colorectal cancer

Introduction

Most human colorectal cancers have mutations in the adenomatous polyposis coli (*APC*) gene or β-catenin gene (*CTNNB1*), leading to increased β-catenin protein expression and activation of downstream β-catenin/T-cell factor (Tcf) target genes (Behrens, 2005). These cancers also exhibit marked changes in the expression of Bcl-2 family proteins (Bedi *et al.*, 1995).

Correspondence: Dr RH Dashwood, Weniger 503, Linus Pauling Institute, Oregon State University, Corvallis, OR 97331-6512, USA.
E-mail: Rod.Dashwood@oregonstate.edu
Received 5 September 2006; revised 25 January 2007; accepted 19 February 2007; published online 2 April 2007

Similar findings have been reported in the colon tumors from animals treated with 2-amino-1-methyl-6-phenylimidazo(4,5-*b*)pyridine (PhIP) and 2-amino-3-methylimidazo(4,5-*f*)quinoline (IQ), which are dietary agents that the US National Toxicology Program has classified as 'reasonably anticipated to be human carcinogens'. Indeed, there are a number of similarities between human and rat colon tumors with respect to β-catenin/Tcf signaling and the expression of Bcl-2 family proteins. First, as in the human situation, PhIP- and IQ-induced colon tumors in the rat contain mutations in *Apc* or *Ctnnb1*, but not in both of these genes (Dashwood *et al.*, 1998). Second, these mutations stabilize β-catenin through inhibition of phosphorylation, ubiquitination and proteasome degradation, leading to increased expression of β-catenin protein (Al-Fageeh *et al.*, 2004). Third, β-catenin/Tcf target genes frequently are overexpressed, including *c-Myc* (Blum *et al.*, 2001, 2003). Fourth, during the progression from normal colonic mucosa to adenoma and carcinoma there is an increase in anti-apoptotic Bcl-2 protein and loss of proapoptotic Bax (Hayashi *et al.*, 1996).

These findings allowed us to ask whether changes in apoptosis-related proteins, and specifically Bcl-2, might be directly related to β-catenin/Tcf signaling. Cloning and characterization studies ruled out the rat *Bcl-2* gene as a direct target of β-catenin, but c-Myc and the transcription factor E2F1 were identified as intermediates in the upregulation of rat *Bcl-2*.

Results

The ratio of Bcl-2/Bax mRNA is increased in PhIP-induced colon tumors containing β*-catenin mutations*

Previous work showed elevated Bcl-2 and decreased Bax protein levels in heterocyclic amine-induced colon tumors (Hayashi *et al.*, 1996); thus, we first examined the expression of *Bcl-2* and *Bax* mRNA in six PhIP-induced colon tumors. Results are summarized in Table 1 in terms of the *Bcl-2/Bax* ratio, together with the mutation status of β-catenin, as determined by polymerase chain reaction-single strand conformation polymorphism (PCR-SSCP) analysis. Codons 32 and 34 of *Ctnnb1* are known 'hot spots' for heterocyclic amine-induced mutation (Dashwood *et al.*, 1998; Blum *et al.*,

Table 1 *Bcl-2/Bax* expression and β-catenin mutation status in PhIP-induced colon tumors

Tumor ID #	*Relative* Bcl-2 *mRNA expression*[a]	*Relative* Bax *mRNA expression*[a]	Bcl-2/Bax *ratio*	Ctnnb1 *mutation status*[b]
98-01-18	4.0	0.5	8	GGA→GAA (G34E)
98-02-16	0.5	1.0	0.5	None detected
98-02-18	4.0	0.5	8	GGA→GAA (G34E)
98-02-20	4.0	0.5	8	GGA→GTA (G34V)
98-02-22	1.0	1.0	1	None detected
98-02-23	1.0	1.0	1	None detected

Abbreviations: PhIP, 2-amino-1-methyl-6-phenylimidazo(4,5-*b*)pyridine. [a]Tumor versus adjacent normal-looking tissue. [b]detected by PCR-based single strand conformation polymorphism analysis and direct sequencing (Dashwood *et al.*, 1998), data not presented. *Ctnnb1*, gene designation for rat β-catenin.

2003), and three PhIP-induced colon tumors had β-catenin GGA→GAA (G34E) or GGA→GTA (G34V) mutations. Although such mutations do not substitute critical Ser/Thr residues directly, they nonetheless stabilize the β-catenin protein by interfering with the relative extent of Ser33 phosphorylation by glycogen synthase kinase-3β (GSK-3β) and subsequent ubiquitination/proteasome degradation (Al-Fageeh *et al.*, 2004). No β-catenin mutations were detected in three other colon tumors (Table 1). Interestingly, tumors with β-catenin mutations had an 8-fold increase in *Bcl-2* versus *Bax* expression, whereas tumors that were wild-type for β-catenin had no marked changes in *Bcl-2* or *Bax*. This suggested that β-catenin might upregulate *Bcl-2* gene expression through direct or indirect mechanisms.

Cloning and characterization of the rat Bcl-2 *5′-flanking sequence*

To investigate whether *Bcl-2* might be a direct β-catenin/Tcf target gene in the rat, we cloned a 1745 bp fragment of the 5′-flanking region of rat *Bcl-2*, also containing part of exon 1 (see GenBank accession no. AF531426). Analysis using MatInspector (Genomatix) revealed putative DNA-binding sites for E2F1, NFκB, AP-2, SP1, c-Myb, SMAD, GATA, PAX3 and other transcription factors. Interestingly, four putative Tcf binding sites also were predicted.

In 5′-RACE experiments, fresh poly(A)$^+$ RNA (Ambion, Austin, TX, USA) consistently generated a single 260-bp product and no larger or smaller fragments, suggesting only full-length poly(A)$^+$ RNAs were amplified (Figure 1a). Moreover, following gel purification and sequence analysis (Figure 1b), the transcription start site was readily assigned to a C nucleotide 231 bp upstream of the translation start site ATG, with a similar genomic organization as human *Bcl-2* (Figure 1e). Indeed, h*Bcl-2* and r*Bcl-2* share 70.1% similarity, and the core promoter region of r*Bcl-2* has 85% identity with h*Bcl-2*, containing several GC boxes, and CAAT and TATA box motifs located close to the AUG translation start site, as in h*Bcl-2* (Harigai *et al.*, 1996).

In human embryonic kidney (HEK) 293 cells (Figure 1c), transient transfection of a reporter fragment containing −1945 to −906 of rat *Bcl-2* (designated hereafter as 'P1') showed 10 times higher promoter activity than the fragment between −905 and −1 (referred to hereafter as 'P2'). Sequential deletion analysis showed that deletion at position −1201 (F7-1) or shorter resulted in significant loss of *Bcl-2* promoter activity (Figure 1d). However, F8-1, F9-1 and F10-2 had high promoter activity, indicating that the core promoter is located between −1201 and −1489 bp. Interestingly, F10-1 had lower promoter activity than F9-1 and F10-2, suggesting that negative regulatory element(s) might exist at each end of the *Bcl-2* promoter.

Identification of transcription factors bound to the rat Bcl-2 *promoter*

Nuclear proteins bound to the rat *Bcl-2* promoter were purified by DNA pull-downs (Zeng *et al.*, 2003), and they were identified using protein/DNA arrays, as reported before (Li *et al.*, 2004). In Array I (Figure 2a), strong signals were obtained for E2F1 (dotted box), NFκB, MEF1, CBF, USF1, c-Myb, NF-1, Pax5 and Smad3/4. There also were signals for AP-1, AP-2, p53, GATA and CREB. In Array II, strong signals were detected for GATA3, ISRE, PARP, RREB2, Pax3 and ZIC (Figure 2b). However, no Tcf signal was observed (Figure 2b, box), even though four putative Tcf sites were predicted using MatInspector software.

Subsequently, mobility-shift assays were performed with ^{32}P-labeled oligos containing one of the four putative Tcf sites, *in vitro* translated Tcf4 (or Lef1), and nuclear extracts from HEK 293 cells. Promising bands initially were observed, but excess cold oligo failed to produce the expected competition, and no supershift was seen with Tcf4 or Lef1 antibodies (data not shown). Taken together with the protein/DNA analyses (Figure 2b), we concluded that the putative Tcf sites in rat *Bcl-2* were not authentic.

E2F1 is a transcriptional activator of rat Bcl-2

Because no authentic Tcf sites were found, 10 different transcription factors with affinity for the rat *Bcl-2* promoter in protein/DNA arrays (Figure 2) were tested for their effects on *Bcl2*-P1. A striking response was seen with E2F1, which increased promoter activity > 10-fold (Figure 3a). Reporter assays were performed with deletion constructs containing two, one, or zero E2F sites in the rat *Bcl-2* promoter (Figure 3b). Exogenous E2F1 increased reporter activities 7- to 11-fold with constructs containing both E2F sites, but there was no effect with constructs containing one or no E2F sites. Site-directed mutagenesis targeted at both E2F sites completely abolished the induction of *Bcl-2* promoter activity by exogenous β-catenin, and the response was markedly attenuated by mutation of site 1, but not site 2 (Figure 3c). Thus, site 1 appears to be more important for β-catenin- or E2F1-induced activation of the *Bcl-2* promoter.

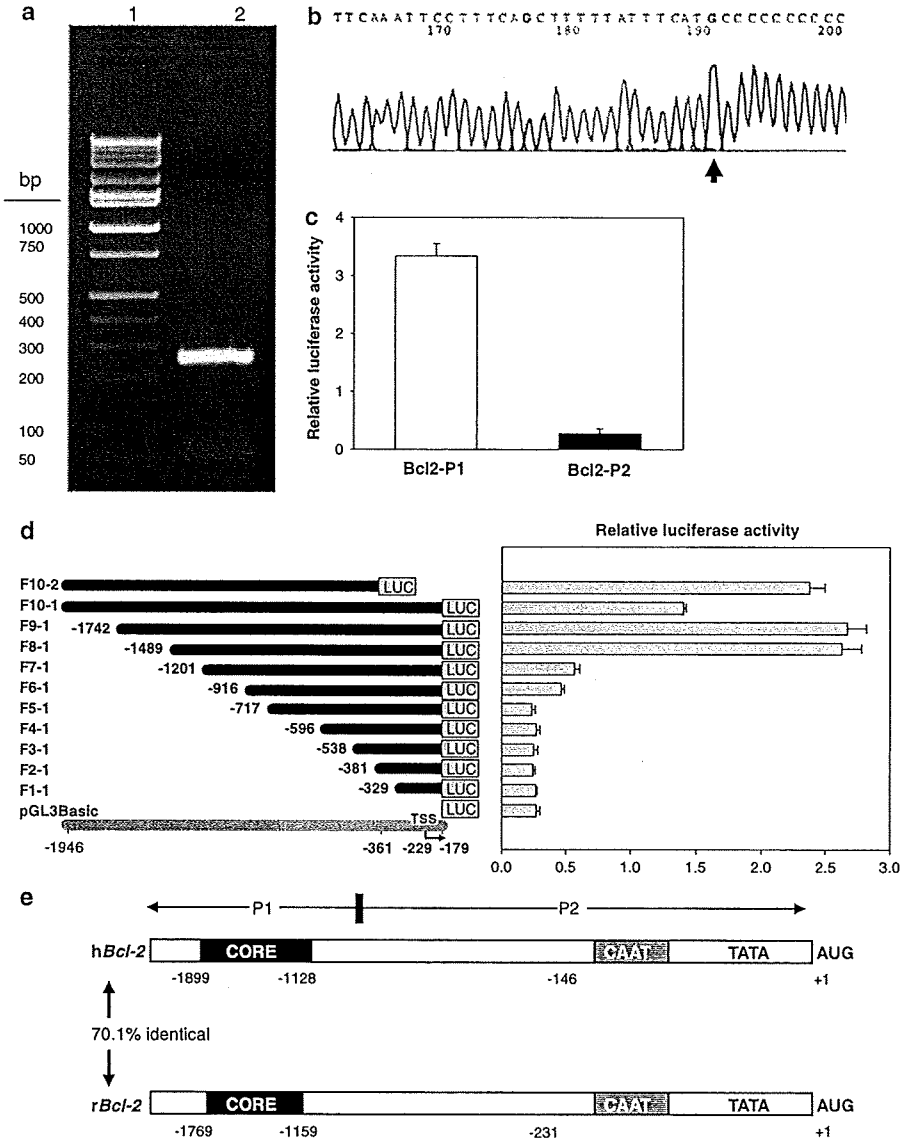

Figure 1 Characterization of the rat Bcl-2 promoter. (a) Product from 5′-rapid amplification of cDNA ends (5′-RACE) on a 2% agarose gel stained with ethidium bromide. In 5′-RACE, fresh poly(A)$^+$ RNA (Ambion) was used to ensure a high percentage of full-length transcripts, which consistently generated a *single* 260 bp PCR product (lane 2; lane 1 = marker ladder). Degradation of full-length poly(A)$^+$ RNAs was discounted based on the lack of shorter or longer 5′-RACE products in repeat experiments, and DNA sequencing (GenBank accession no. AF531426) indicated a common 5′ end with the major TSS assigned to a C nucleotide 231 bp upstream of the translation start site (b), consistent with the human *BCL-2* counterpart. (c) *Bcl-2* promoter-luciferase reporter construct containing promoter region P1 had >10-fold higher activity than region P2 when transfected into HEK293 cells and luciferase activities were measured in whole cell lysates 48 h post-transfection. (d) Deletion analysis. Left panel: schematic view of *Bcl-2* promoter-luciferase reporter constructs; gray line, position in genomic DNA sequence; bent arrow, transcription start site (TSS); black lines, extent of genomic DNA attached to the luciferase (LUC) gene. Promoter fragments were designated as F1-1 through F10-2, as shown at left. Right panel: *Bcl-2* promoter activity in HEK293 cells. Transcriptional activity was evaluated by transient transfection, using the constructs shown in the left panel. Cells were extracted using 1 × Reporter lysis buffer, 48 h post-transfection. Values represent the mean ± s.d. of three independent transfections for each construct, normalized for transfection efficiency using pSV-β-Gal, as reported before (Li *et al*., 2004). (e) Genomic organization of human *BCL-2* (h*BCL-2*) and rat *Bcl-2* (r*Bcl-2*) promoters, with numbering relative to the translation start codon (AUG). CORE, core promoter region.

β-*Catenin upregulates* Bcl-2 *promoter activity*

Although *Bcl-2* was excluded as a direct target of β-catenin, owing to the lack of authentic Tcf sites (see above), we observed induction of *Bcl-2*-P1 reporter activity after forced expression of β-catenin. Thus, in HEK293 cells, overexpression of wild-type β-catenin by transient transfection increased the reporter activity twofold (Figure 4a), and LiCl, a well-known inhibitor of GSK-3β that stabilizes endogenous β-catenin (Aberle *et al*., 1997; Al-Fageeh *et al*., 2004), also increased *Bcl-2*

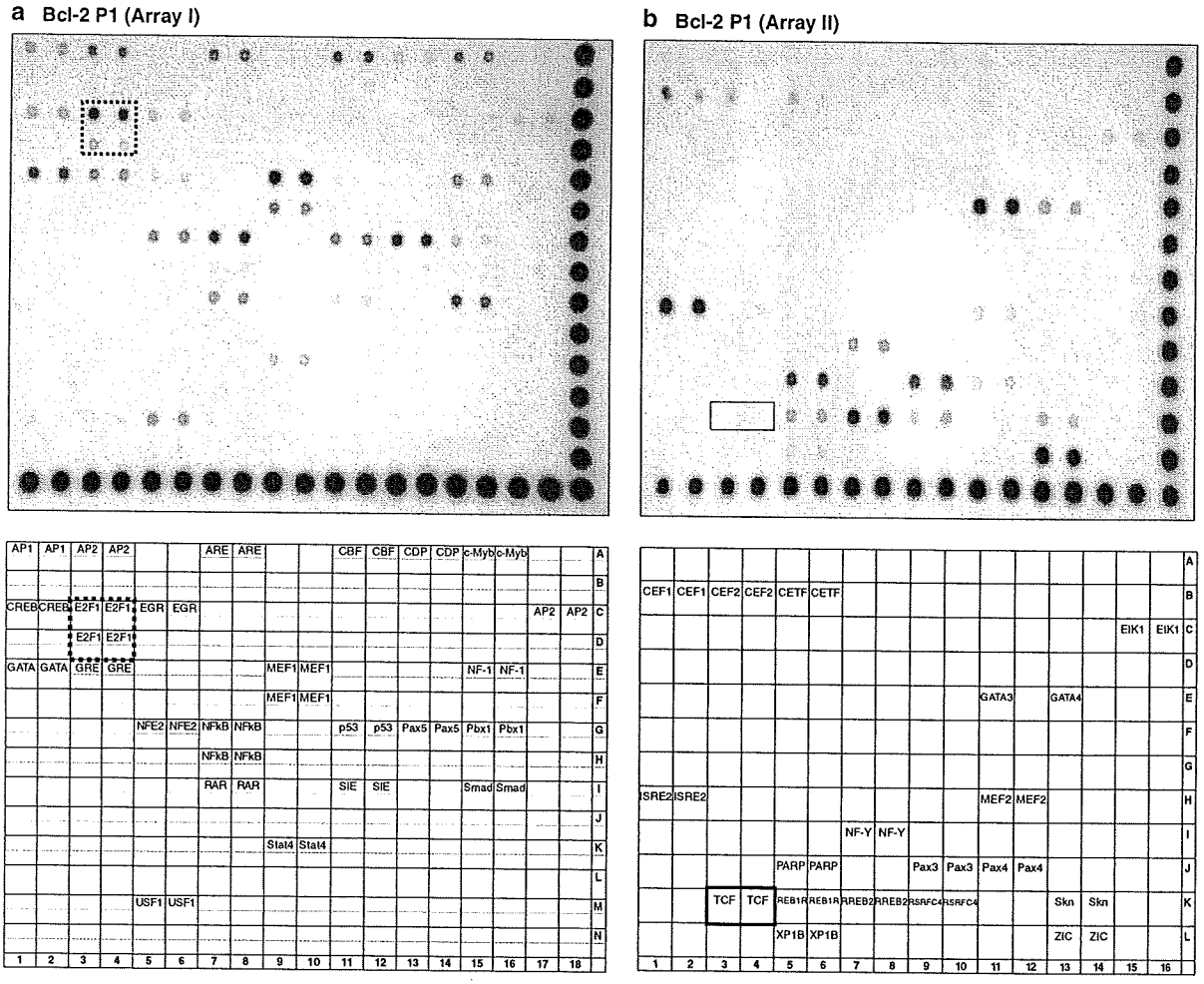

Figure 2 Transcription factors bound to the rat *Bcl-2* promoter. Nuclear proteins bound to a 1040 bp (−1945 to −906) fragment of r*Bcl-2* promoter region P1 were pulled down from nuclear extracts of HEK293 cells and transcription factors were identified using TranSignal protein/DNA Array I (a) and Array II (b) (Panomics), as reported (Li *et al.*, 2004). Top panels, hybridization signals; bottom panels, transcription factor identities. Box, Tcf signal; dotted box, E2F1 signal.

promoter activity. Immunoblotting of whole cell lysates confirmed that β-catenin and Bcl-2 proteins were increased by exogenous β-catenin and LiCl treatment (Figure 4b). Rather than using other means to increase endogenous wild-type β-catenin, such as soluble Wnt3a (Park *et al.*, 2006), we examined oncogenic mutants found in PhIP-induced colon tumors, namely D32N, G34E and Δ45 (Figure 4c). Each β-catenin mutant activated *Bcl-2* reporter activity more effectively than wild-type β-catenin, and there was a concomitant increase in Bcl-2 and β-catenin protein expression in cell lysates.

β-*Catenin upregulates c-Myc, E2F1 and hence Bcl-2*

Because c-Myc is a well-known direct target of β-catenin/Tcf signaling (He *et al.*, 1998), we next used siRNA to knockdown c-Myc. Overexpression of β-catenin induced rat *Bcl-2* promoter activity (Figure 5a, upper panel), and increased protein expression of c-Myc, E2F1 and Bcl-2 (Figure 5a, lower panel). Reduction of c-Myc by siRNA blocked β-catenin-dependent induction of rat *Bcl-2* promoter activity, as well as E2F1 and Bcl-2 protein expression. These data confirmed that c-Myc is not only a β-catenin/Tcf target, but also an E2F1 activator. Finally, using siRNA to knockdown E2F1 (Figure 5b), there was a corresponding attenuation of *Bcl-2* promoter activity and Bcl-2 protein expression, with more cells undergoing apoptosis, as evidenced by an increased in cleaved (active) caspase-3.

Discussion

Elevated expression of β-catenin has been detected in colorectal and other cancers, resulting in constitutive activation of numerous β-catenin/Tcf target genes (Behrens, 2005). We reported on the high frequency of

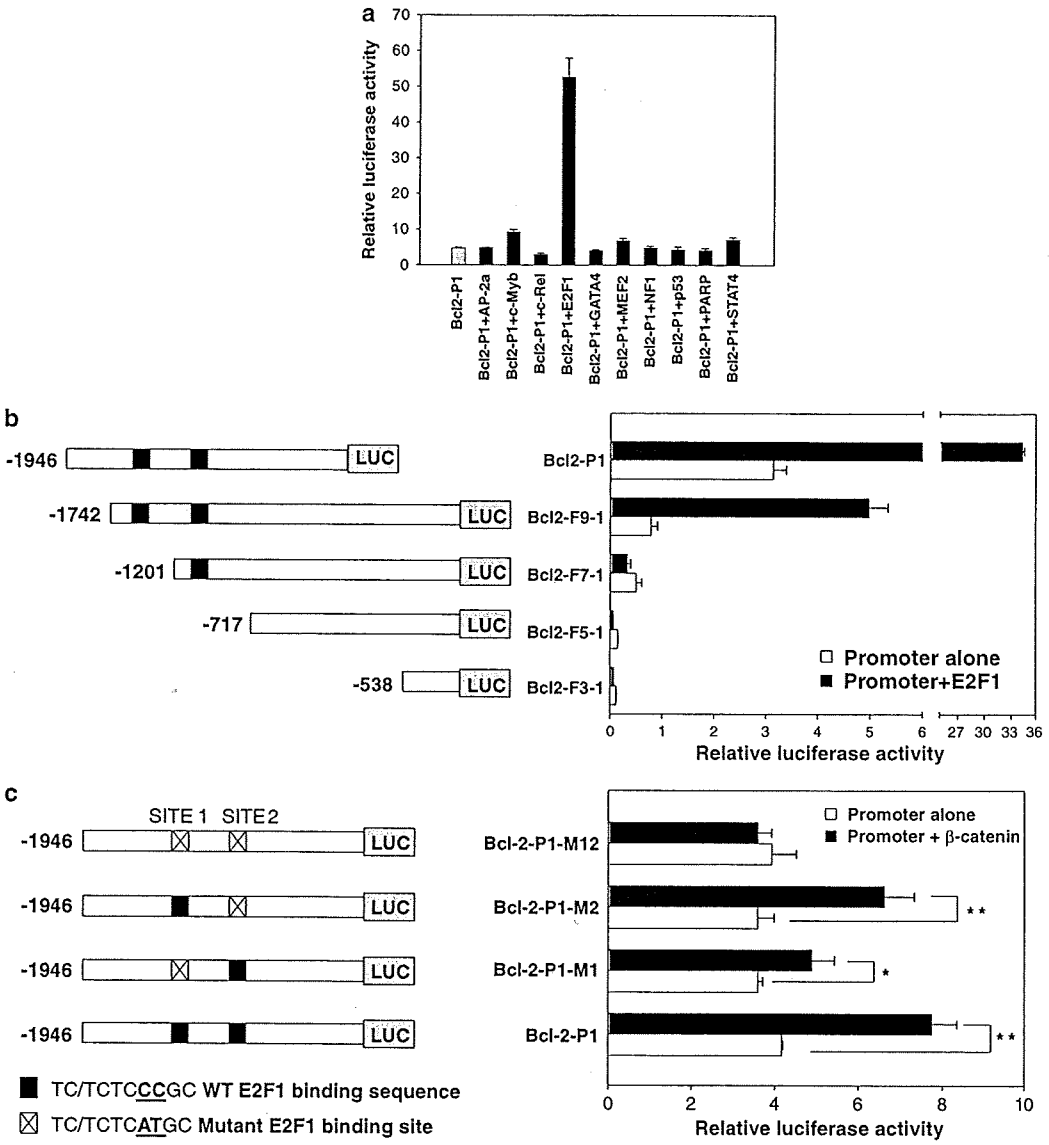

Figure 3 Confirmation of E2F1 sites in the rat *Bcl-2* promoter. (a) HEK293 cells were transfected with *Bcl-2*-P1 plus constructs expressing transcription factors identified in protein-DNA arrays (Figure 2). pSV-β-Gal was used as internal control. Cell lysates were analyzed for luciferase and β-Gal activities 48 h post-transfection. Luciferase activity was normalized to β-Gal to obtain the relative luciferase activity. E2F-1 binding sites were confirmed using (b) deletion analyses and (c) site-directed mutagenesis. Left, diagram of *Bcl-2* promoter-luciferase constructs. Right, *Bcl-2* promoter activities in the presence and absence of exogenous (b) E2F1 or (c) β-catenin. Data, mean ± s.d., $n=3$. WT, wild-type. $^{*}P<0.05$; $^{**}P<0.01$.

β-catenin mutations in PhIP- and IQ-induced rat colon tumors (Dashwood *et al.*, 1998), the overexpression of β-catenin/Tcf targets such as c-Myc and c-Jun (Blum *et al.*, 2001), and the elevated expression of Bcl-2 protein with loss of Bax (Hayashi *et al.*, 1996). In the present investigation of PhIP-induced colon tumors, a striking concordance was found between the presence of β-catenin mutations and increased *Bcl-2*/*Bax* mRNA expression (Table 1), suggesting that β-catenin/Tcf might activate the rat *Bcl-2* gene (and/or inhibit Bax) at the transcriptional level.

The *Bcl-2* proto-oncogene is frequently expressed in human cancers, and Bcl-2 is regulated both transcriptionally and post-transcriptionally (Bedi *et al.*, 1995; Harigai *et al.*, 1996). We cloned and characterized the rat *Bcl-2* promoter for the first time and found a similar genomic organization as the human counterpart, *BCL-2* (Seto *et al.*, 1988; Harigai *et al.*, 1996), with a core promoter that shares 85% identity between the two species. We also identified transcription factors bound to the rat *Bcl-2* promoter, and excluded several putative Tcf sites on the basis of the results from protein/DNA

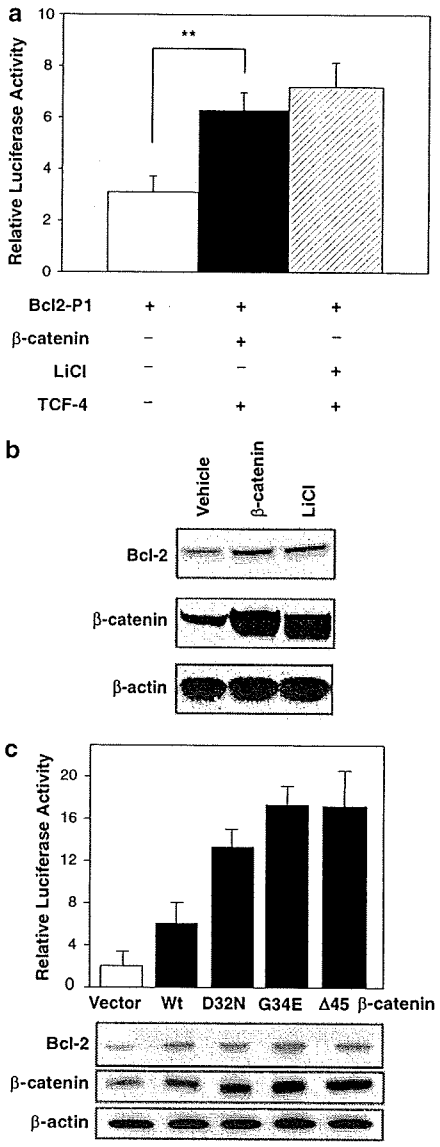

Figure 4 Regulation of *Bcl-2* promoter activity by β-catenin. (a) Induction of *Bcl-2* promoter activity by forced expression of β-catenin. HEK293 cells were transfected with *Bcl-2*-P1 promoter-luciferase construct alone, or *Bcl-2*-P1 plus a construct that overexpressed wild-type β-catenin; pSV-β-Gal was used as internal control. Alternatively, endogenous β-catenin was overexpressed with 30 mM LiCl. (b) Immunoblot of whole cell lysates showing increased Bcl-2 and β-catenin following exogenous β-catenin or LiCl treatment. (c) Induction of *Bcl-2* promoter–reporter activity by wild-type (Wt) β-catenin and β-catenin mutants D32N, G34E and Δ45, with concomitant changes in β-catenin and Bcl-2 protein expression in whole cell lysates.

arrays (Figure 2) and mobility-shift assays (data not shown). Thus, the rat *Bcl-2* gene does not appear to be a direct β-catenin/Tcf target.

Various transcription factors have been implicated as regulators of Bcl-2 (Wilson *et al*., 1996; Salomoni *et al*., 1997; Smith *et al*., 1998; Mayo *et al*., 1999; Pugazhenthi *et al*., 1999; Romero *et al*., 1999; Tamatani *et al*., 1999; Grossmann *et al*., 2000). Human *BCL-2* contains an authentic E2F response element (Gomez-Manzano *et al*., 2001) and was identified as an E2F1 target gene by cDNA microarray analysis (Muller *et al*., 2001). We report here, for the first time, that E2F1 also directly regulates the rat *Bcl-2* gene, with strong signals in protein/DNA arrays (Figure 2) and loss of promoter activity upon deletion of the E2F1 sites (Figure 3).

Rat *Bcl-2* promoter activity was increased by LiCl treatment and by exogenous wild-type and mutant β-catenins. Lithium has been shown to stabilize β-catenin via inhibition of GSK-3β (Behrens, 2005), and increased Bcl-2 levels in rat frontal cortex, hippocampus and striatum, as well as in cultured retinal ganglion cells (Manji *et al*., 2000; Huang *et al*., 2003). Of particular interest, however, oncogenic mutants of β-catenin from PhIP-induced colon tumors strongly activated *Bcl-2* promoter activity and Bcl-2 protein expression, supporting a link between increased β-catenin and Bcl-2 (Figure 4c).

c-*Myc* is a well-known β-catenin/Tcf target (He *et al*., 1998), and is strongly overexpressed in rat colon tumors both at the mRNA and protein level (Blum *et al*., 2001; Fujiwara *et al*., 2004). Interestingly, a recent report indicated that c-Myc-regulated microRNAs modulate E2F1 expression (O'Donnell *et al*., 2005). In our experiments, knockdown of c-Myc by siRNA blocked the induction of E2F1 and Bcl-2 by β-catenin, as well as inhibiting rat *Bcl-2* promoter activity (Figure 5a), and knockdown of E2F1 by siRNA also attenuated *Bcl-2* reporter activity and Bcl-2 protein expression (Figure 5b). We conclude that an indirect pathway exists between β-catenin and Bcl-2 in PhIP-induced colon tumors, in which mutations in β-catenin activate β-catenin/Tcf signaling, increase c-Myc, elevate E2F1 expression and enhance Bcl-2 expression. Further studies of this pathway are warranted, including the possible contribution of miroRNAs in PhIP-induced colon tumors and early lesions such as colonic aberrant crypts and dysplastic foci (Ochiai *et al*., 2003).

Materials and methods

Source of colon tumors

Colon tumors were from a study in which male F344 rats were treated with PhIP, as reported previously (Dashwood *et al*., 1998). At necropsy, one portion of each tumor was taken for histopathology, and other portions were frozen in liquid nitrogen for molecular analyses.

Competitive RT-PCR

Total RNA was isolated from colon tumors and adjacent normal looking tissue using RNeasy RNA isolation kit (Qiagen, Valencia, CA, USA). cDNAs were amplified with primers specific for *Bcl-2* or *Bax* in the presence of serial dilutions of competitor DNA (Clontech, Palo Alto, CA, USA). Parallel reactions were run with primers and competitor DNA for the housekeeping gene glyceraldehyde-3-phosphate dehydrogenase (*GAPDH*). PCR products were separated on 2% agarose gels, visualized by ethidium bromide staining and

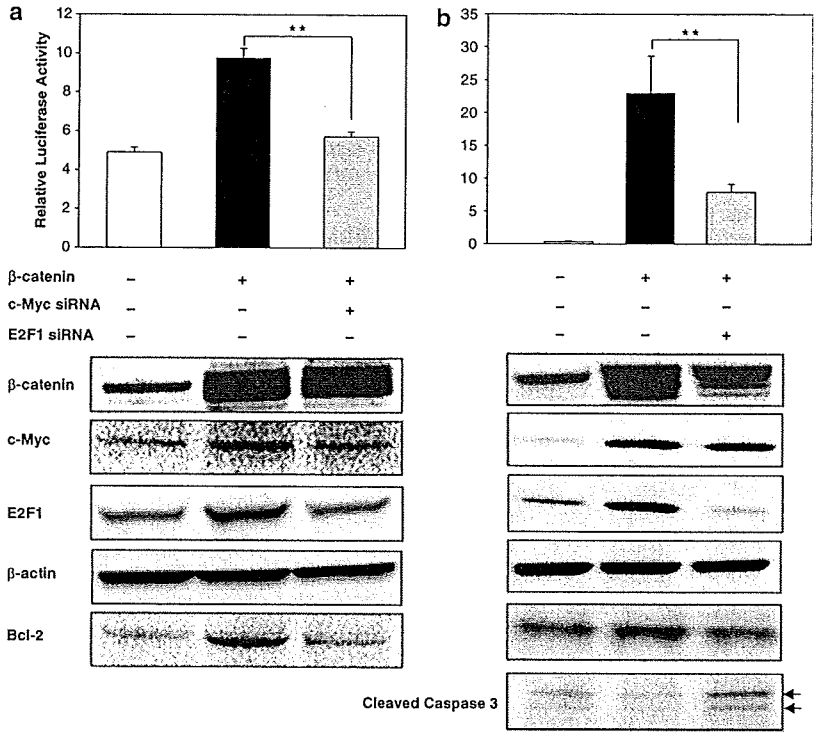

Figure 5 Knockdown of c-Myc or E2F1 attenuates β-catenin-dependent induction of *Bcl-2* promoter activity and Bcl-2 protein expression. HEK293 cells were transfected with *Bcl-2*-P1, in the presence and absence of exogenous β-catenin, plus c-Myc siRNA or E2F1 siRNA. Luciferase and β-Gal activities were assayed 48 h post-transfection. Luciferase activity was normalized to β-Gal activity to obtain the Relative Luciferase Activity. Data, mean ± s.d., $n=3$; $^{**}P<0.01$. Corresponding whole cell lysates were immunoblotted for β-catenin, c-Myc, E2F1, β-actin, Bcl-2 and cleaved caspase 3, as indicated. Arrows, 19-kDa and 17-kDa bands indicative of cleaved (active) caspase 3.

quantified on an AlphaImager 2200 (AlphaInnotech, San Leandro, CA, USA). *Bcl-2* or *Bax* levels, normalized relative to *GAPDH*, were expressed for tumor versus normal looking tissue.

Mutation screening

PhIP-induced colon tumors and adjacent normal looking tissue were subjected to DNA isolation and PCR-based single strand conformation polymorphism (PCR-SSCP) analyses, using the experimental conditions reported previously (Dashwood *et al*., 1998).

Cloning of the 5′-flanking region of Bcl-2

The 5′-flanking region of the rat *Bcl-2* gene was amplified using the Rat GenomeWalker kit (Clontech). The primary PCR was performed with Adapter Primer 1, supplied with the kit and gene-specific primer rBcl2P-GSP1 (5′-TGCATTCT TG GATGAAGGGGTGTCTT-3′). Subsequently, secondary PCR was performed with Adapter Primer 2 (supplied with the kit) and a nested gene-specific primer rBcl2P-GSP2 (5′-TCCCCCTTGGCATGAGATGCAGGAAAT-3′). The primary PCR was performed for 35 cycles at 98°C for 20 s and 65°C for 4 min, with an additional 10 min extension at 72°C after the final cycle. The nested PCR was run for 30 cycles, denaturing for 20 s at 98°C, annealing for 5 min at 68°C, and ending with a final extension for 10 min at 72°C. PCR products were subcloned into pGEM-T (Promega, Madison, WI, USA) and subjected to DNA sequencing in both directions on an ABI Prizm model 377 sequencer (Applied Biosystems, Bedford, MA, USA). Based on the new sequence, primers rBcl2P-GSP3 (5′-GGGAACGGGGACCAGAATCCTCTTCT-3′) and rBcl2P-GSP4 (5′-TTAAACTCCGAAGGGCCAATGCG TTTTC-3′) were used to obtain additional flanking sequence of *Bcl-2*.

5′-Rapid amplification of cDNA ends (5′-RACE)

The transcription start site was identified using 5′-RACE System Version 2.0 (Invitrogen, Carlsbad, CA, USA), according to the manufacturer's protocol. First strand cDNA was synthesized from 100 ng rat liver poly(A)$^+$ RNA using an antisense gene-specific primer RA-b2-GSP1 (5′-CCTCT GTGACAGCTTAT-3′). The cDNA was purified and an oligo-dC tail was added to the 3′ end of the cDNA using terminal transferase TdT. Homopolymeric C tailed cDNA was then amplified by PCR using Abridged Anchor Primer (supplied with the kit) and a nested gene-specific primer RA-b2-GSP2 (5′-CGGTTATCATACCCTGTTCTCCCGGCTT-3′). PCR tubes were transferred from ice to a thermal cycler pre-equilibrated to 94°C, and after 2–3 min 35 cycles were performed of 30 s/94°C, 30 s/55°C and 60 s/72°C, with final extension at 72°C for 10 min. The PCR product was further amplified using nested primers AUAP (supplied with the kit) and RA-b2-GSP3 (5′-GAAGCTGCAGGTACCAATAGCA CTT-3′), and cycling parameters identical to the first round.

5′-RACE products were purified using Wizard PCR Preps DNA Purification System (Promega) and sequenced using primer RA-b2-GSP3.

Construction of Plasmids
Progressive deletion constructs of the rat *Bcl-2* promoter, including Bcl2-P1 (−1945 to −906) and Bcl2-P2 (−905 to −1), were engineered by cloning PCR fragments between *Kpn*I and *Xho*I sites of the reporter luciferase vector pGL3Basic (Promega); primer sequences are available upon request. Plasmids containing one or two mutant E2F1-binding sites were generated from pGL3-Bcl2-P1 by site-directed mutagenesis using the QuickChange II XL site-directed mutagenesis kit (Stratagene, La Jolla, CA, USA). To generate pcDNA3.1-E2F1, an E2F1 expression construct, full-length human E2F1 cDNA was amplified by RT-PCR. The PCR products were cloned into pcDNA3.1(+) (Invitrogen, Carlsbad, CA, USA) between *Bam*HI and *Eco*RV sites. According to the same methodology, plasmids expressing AP2α, c-Rel, c-Myb, GATA4, MEF2, NF-1, p53, PARP and STAT4 were constructed by subcloning the corresponding full-length cDNA into pcDNA3.1(+). The wild-type β-catenin cDNA construct pcDNAI/β-catenin was kindly provided by Hans Clevers and Marc van de Wetering. Oncogenic β-catenin mutants, generated by fragment switching, were as described before (Dashwood *et al*., 2002; Al-Fageeh *et al*. 2004; Dashwood *et al*., 2005). All constructs were confirmed by sequencing in both directions.

c-Myc and E2F1 knockdown by siRNA
Inhibition of c-Myc expression in HEK293 cells was performed using SureSilencing Human MYC siRNA and Antibody Kit (SuperArray Biosciences, Frederick, MO, USA). Cells were transfected with MYC-specific siRNA population using Lipofectamine2000 (Invitrogen) as recommended by the manufacturer. Non-specific siRNA was used as negative control. In subsequent experiments, E2F1 was knocked down using ON-TARGETplus SMARTpool human E2F1 siRNA from Dharmacon (Chicago, IL, USA).

Cell culture and transient transfection experiments
HEK293 cells were grown in Dulbecco's modified Eagle's medium (DMEM) supplemented with 10% horse serum (Invitrogen). Rat kidney epithelial (RK3E) cells were grown in DMEM supplemented with 10% bovine fetal serum (Invitrogen). Cultures were maintained at 37°C in a humidified 5% CO_2-containing atmosphere. Transfection was performed using TransFast (Promega) or FuGENE 6 (Roche, Palo Alto, CA, USA) following manufacturer's instructions, and cells were harvested 48 h after transfection. To inhibit GSK-3β and induce endogenous β-catenin, 30 mM LiCl was added to culture medium; 30 mM NaCl was used as control.

β-Galactosidase (β-Gal) and luciferase assays
β-Galactosidase and luciferase assays were performed as reported previously (Li *et al*., 2004).

Isolation of transcription factors bound to the rat Bcl-2 *promoter*
Transcription factors bound to the 1040 bp *Bcl-2* promoter 1 (−1945 to −906) were purified by DNA pull-down assays according to the procedure described previously (Li *et al*., 2004). *Bcl-2* promoter fragments were end labeled with biotin using Bio-16-dUTP (Enzo Life Sciences, Farmingdale, NY, USA) and the Klenow fragment of DNA polymerase I (Fermentas Inc., Hanover, MD, USA). Proteins were eluted on ice in 50 μl of TGED buffer containing 2 M NaCl.

Protein/DNA array analyses
After DNA pull-down assays, TranSignal Protein/DNA Arrays I and II (Panomics, Redwood, CA, USA) were used to identify the transcription factors associated with the rat *Bcl-2* promoter, as described before for the β-catenin gene *Ctnnb1* (Li *et al*., 2004).

Western blotting
Whole cell lysates were prepared using Reporter Lysis buffer (Promega) and the protein concentration was determined as reported (Li and Dashwood, 2004; Li *et al*., 2004). Proteins were separated on 4–12% bis-tris gels (Novex, Invitrogen) and transferred to nitrocellulose membranes (Invitrogen), and after incubation with primary antibody followed by secondary antibody conjugated to horseradish peroxidase, detection was by Western Lighting Chemiluminescence Reagents Plus (Perkin Elmer Life Science, Boston, MA, USA).

Acknowledgements

Minako Nagao and Hideaki Inamori are gratefully acknowledged for their help in the studies with PhIP-induced colon tumors, which were supported by a fellowship from the Foundation for Promotion of Cancer Research, Tokyo, Japan. We thank Mark van de Wetering and Hans Clevers of University Hospital Utrecht, The Netherlands, for the wild-type β-catenin construct. This work was supported by NIH grants CA65525, CA80176 and CA90890, and by NIEHS center grant P30 ES00210.

References

Aberle H, Bauer A, Stappert J, Kispert A, Kemler R. (1997). β-catenin is a target for the ubiquitin-proteasome pathway. *EMBO J* **16**: 3797–3804.

Al-Fageeh M, Li Q, Dashwood WM, Myzak MC, Dashwood RH. (2004). Phosphorylation and ubiquitination of oncogenic mutants of β-catenin containing substitutions at Asp32. *Oncogene* **23**: 4839–4846.

Bedi A, Pasricha PJ, Akhtar AJ, Barber JP, Bedi GC, Giardiello FM *et al*. (1995). Inhibition of apoptosis during development of colorectal cancer. *Cancer Res* **55**: 1811–1816.

Behrens J. (2005). The role of the Wnt signalling pathway in colorectal tumorigenesis. *Biochem Soc Trans* **33**: 672–675.

Blum CA, Xu M, Orner GA, Fong AT, Bailey GS, Stoner GD *et al*. (2001). β-Catenin mutation in rat colon tumors initiated by 1,2-dimethylhydrazine and 2-amino-3-methylimidazo[4,5-*f*]quinoline, and the effect of post-initiation treatment with chlorophyllin and indole-3-carbinol. *Carcinogenesis* **22**: 315–320.

Blum CA, Tanaka T, Zhong X, Li Q, Dashwood WM, Pereira C *et al*. (2003). Mutational analysis of *Ctnnb1* and *Apc* in tumors from rats given 1,2-dimethylhydrazine or 2-amino-3-methylimidazo[4,5-*f*]quinoline: mutational 'hotspots' and the relative expression of β-catenin and c-jun. *Mol Carcinogen* **36**: 195–203.

Dashwood RH, Suzui M, Nakagama H, Sugimura T, Nagao M. (1998). High frequency of β-catenin (*Ctnnb1*) mutations in the colon tumors induced by two heterocyclic amines in the F344 rat. *Cancer Res* **58**: 1127–1129.

Dashwood WM, Orner GA, Dashwood RH. (2002). Inhibition of β-catenin/Tcf activity by white tea, green tea, and epigallocatechin-3-gallate (EGCG): minor contribution of H_2O_2 at physiologically relevant EGCG concentrations. *Biochem Biophys Res Commun* **296**: 584–588.

Dashwood WM, Carter O, Al-Fageeh M, Li Q, Dashwood RH. (2005). Lysosomal trafficking of β-catenin induced by the tea polyphenol epigallocatechin-3-gallate. *Mutat Res* **591**: 161–172.

Fujiwara K, Ochiai M, Ohta T, Ohki M, Aburatani H, Nagao M *et al.* (2004). Global gene expression analysis of rat colon cancers induced by a food-borne carcinogen, 2-amino-3-methylimidazo[4,5-*f*]quinoline. *Carcinogenesis* **25**: 1495–1505.

Gomez-Manzano C, Mitlianga P, Fueyo J, Lee HY, Hu M, Spurgers KB *et al.* (2001). Transfer of E2F-1 to human glioma cells results in transcriptional up-regulation of Bcl-2. *Cancer Res* **61**: 6693–6697.

Grossmann M, O'Reilly LA, Gugasyan R, Strasser A, Adams JM, Gerondakis S. (2000). The anti-apoptotic activities of Rel and RelA required during B-cell maturation involve the regulation of Bcl-2 expression. *EMBO J* **19**: 6351–6360.

Harigai M, Miyashita T, Hanada M, Reed JC. (1996). A cis-acting element in the *BCL-2* gene controls expression through translational mechanisms. *Oncogene* **12**: 1369–1374.

Hayashi R, Luk H, Horio D, Dashwood RH. (1996). Inhibition of apoptosis in colon tumors induced in the rat by 2-amino-3-methylimidazo[4,5-*f*]quinoline. *Cancer Res* **56**: 4307–4310.

He TC, Sparks AB, Rago C, Hermeking H, Zawel L, da Costa LT *et al.* (1998). Identification of c-MYC as a target of the APC pathway. *Science* **281**: 1509–1512.

Huang X, Wu DY, Chen G, Manji H, Chen DF. (2003). Support of retinal ganglion cell survival and axon regeneration by lithium through a Bcl-2-dependent mechanism. *Invest Ophthalmol Vis Sci* **44**: 347–354.

Li Q, Dashwood WM, Zhong X, Al-Fageeh M, Dashwood RH. (2004). Cloning of the rat β-catenin gene (*Ctnnb1*) promoter and its functional analysis compared with the *Catnb* and *CTNNB1* promoters. *Genomics* **83**: 231–242.

Li Q, Dashwood RH. (2004). Activator protein-2α associates with adenomatous polyposis coli/β-catenin and inhibits β-catenin/T-cell factor transcriptional activity in colorectal cancer cells. *J Biol Chem* **269**: 45669–45675.

Manji HK, Moore GJ, Chen G. (2000). Lithium up-regulates the cytoprotective protein Bcl-2 in the CNS *in vivo*: a role for neurotrophic and neuroprotective effects in manic depressive illness. *J Clin Psychiatry* **61**: 82–96.

Mayo MW, Wang C, Drouin SS, Madrid LV, Marshall AF, Reed JC *et al.* (1999). WT1 modulates apoptosis by transcriptionally upregulating the bcl-2 proto-oncogene. *EMBO J* **18**: 3990–4003.

Muller H, Bracken AP, Vernell R, Moroni MC, Christians F, Grassilli E *et al.* (2001). E2Fs regulate the expression of genes involved in differentiation, development, proliferation, and apoptosis. *Genes Dev* **15**: 267–285.

Ochiai M, Ushigome M, Fujiwara K, Ubagai T, Kawamori T, Sugimura T *et al.* (2003). Characterization of dysplastic aberrant crypt foci in the rat colon induced by 2-amino-3-methylimidazo[4,5-*f*]quinoline. *Am J Pathol* **163**: 1607–1614.

O'Donnell K, Wentzel EA, Zeller KI, Dang CV, Mendell JT. (2005). c-Myc-regulated microRNAs modulate E2F1 expression. *Nature* **435**: 839–843.

Park S, Gwak J, Cho M, Song T, Won J, Kim DE *et al.* (2006). Hexachlorophene inhibits Wnt/β-catenin pathway by promoting Siah-mediated β-catenin degradation. *Mol Pharmacol* **70**: 960–966.

Pugazhenthi S, Miller E, Sable C, Young P, Heidenreich KA, Boxer LM *et al.* (1999). Insulin-like growth factor-1 induces bcl-2 promoter through a transcription factor cAMP-response element-binding protein. *J Biol Chem* **274**: 2829–2837.

Romero O, Martinez AC, Camonis J, Rebollo A. (1999). Aiolos transcription factor controls cell death in T cells by regulating Bcl-2 expression and its cellular localization. *EMBO J* **18**: 3419–3430.

Seto M, Jaeger U, Hockett RD, Graninger W, Bennett S, Goldman P *et al.* (1988). Alternative promoters and exons, somatic mutation and deregulation of the Bcl-2-Ig fusion gene in lymphoma. *EMBO J* **7**: 123–131.

Salomoni P, Perrotti D, Martinez R, Franceschi C, Calabretta B. (1997). Resistance to apoptosis in CTLL-2 cells constitutively expressing c-Myb is associated with induction of BCL-2 expression and c-MYB-dependent regulation of bcl-2 promoter activity. *Proc Natl Acad Sci USA* **94**: 3296–3301.

Smith MD, Ensor EA, Coffin RS, Boxer LM, Latchman DS. (1998). Bcl-2 transcription from the proximal P2 promoter is activated in neuronal cells by the Brn-3a POU family transcription factor. *J Biol Chem* **273**: 16715–16722.

Tamatani M, Che YH, Matsuzaki H, Ogawa S, Okado S, Miyake S *et al.* (1999). Tumor necrosis factor induces Bcl-2 and Bcl-x expression through NFκB activation in primary hippocampal neurons. *J Biol Chem* **274**: 8531–8538.

Wilson BE, Mochon E, Boxer LM. (1996). Induction of bcl-2 expression by phosphorylated CREB proteins during B-cell activation and rescue from apopotosis. *Mol Cell Biol* **16**: 5546–5556.

Zeng G, Gao L, Xia T, Tencomnao T, Yu RK. (2003). Characterization of the 5′-flanking fragment of the human GM3-synthase gene. *Biochim Biophys Acta* **1625**: 30–35.

Journal of Cellular Biochemistry 101:321–330 (2007)

Induction of Abnormal Nuclear Shapes in Two Distinct Modes by Overexpression of Serine/Threonine Protein Phosphatase 5 in HeLa Cells

Hirokazu Fukuda, Naoto Tsuchiya, Kaori Hara-Fujita, Sachiyo Takagi, Minako Nagao, and Hitoshi Nakagama*

Biochemistry Division, National Cancer Center Research Institute, Tokyo, Japan

Abstract Okadaic acid-sensitve serine/threonine protein phosphatase 5 (PP5) is expressed ubiquitously in various tissues and is considered to participate in many cellular processes. PP5 has a catalytic domain in the C-terminal region and three tetratricopeptide repeat (TPR) motifs in the N-terminal region, which are suspected to function as a protein–protein interaction domain. Physiological roles of PP5 are still largely unknown, although several PP5-binding proteins were reported and a few in vivo functions of PP5 were suggested. In the present study, the effects of expression of the full-length wild-type PP5 fused with EGFP (EGFP-$PP5_{WT}$) and its phosphatase-dead mutant EGFP-$PP5_{H304A}$ were investigated. Transient expression of either EGFP-$PP5_{WT}$ or EGFP-$PP5_{H304A}$ in HeLa cells induced deformed nuclei with a 10-fold frequency compared to that of EGFP. Abnormal-shaped nuclei were also substantially increased by induced moderate expression of PP5 in tet-on HeLa cells. Many HeLa cells expressing EGFP-$PP5_{WT}$ possessed multi-nuclei separated from each other by nuclear membrane, while expression of EGFP-$PP5_{H304A}$ induced deformed nuclei which were multiple-like in shape, but not separated completely and were surrounded by one nuclear membrane. These results suggest that PP5 plays important roles at the M-phase of the cell cycle, especially in separation of chromosomes and formation of nuclear membrane. J. Cell. Biochem. 101: 321–330, 2007. © 2006 Wiley-Liss, Inc.

Key words: PP5; protein phosphatase; abnormal nuclei; deformed nuclei; (E)GFP

Protein phosphatase 5 (PP5) is a member of serine/threonine phosphoprotein phosphatases and is expressed ubiquitously in various tissues. Its cDNA was isolated by the nucleotide sequence similarity of the catalytic domain with that of PP2A and other members of serine/threonine protein phosphatase (PPase) and by a yeast two-hybrid screen to identify proteins interacting with atrial natriuretic peptide (ANP) receptor [Becker et al., 1994; Chen et al., 1994; Chinkers, 1994]. Being distinct from other PPases, PP5 has a unique structural feature and contains three tetratricopeptide repeat (TPR) motifs in the N-terminal region and a catalytic domain in the C-terminal region [for reviews, see Cohen, 1997; Chinkers, 2001]. The TPR motifs are considered to serve as an interface for protein–protein interaction [Lamb et al., 1995]. The TPR domain and C-terminal 11 amino acid residues of PP5 were supposed to be auto-inhibitory domains [Chen and Cohen, 1997; Sinclair et al., 1999; Kang et al., 2001]. The crystal structure of PP5 reported recently proved that the TPR domain blocks the catalytic channel, and the C-terminal residues interact with the TPR domain and stabilize the auto-inhibitory conformation [Yang et al., 2005]. Some unsaturated long-chain fatty acids, including arachidonic acid and long-chain fatty acyl-CoA esters, bind to the N-terminal TPR domain of PP5 and enhance the phosphatase activity *in vitro* [Skinner et al., 1997; Ramsey and Chinkers, 2002]. A recent study showed that arachidonic acid and nocodazole induce the cleavage of the C-terminal of PP5 and stimulate

Abbreviations used: PP5, protein phosphatase 5; TPR, tetratricopeptide repeat; EGFP, enhanced green fluorescence protein; ASK1, apoptosis signal-regulating kinase.

Grant sponsor: The Ministry of Health, Labour and Welfare of Japan; Grant number: 15-12.

*Correspondence to: Hitoshi Nakagama, 1-1, Tsukiji 5, Chuo-ku, Tokyo 104-0045, Japan.
E-mail: hnakagam@gan2.res.ncc.go.jp

Received 20 July 2006; Accepted 28 September 2006
DOI 10.1002/jcb.21178

its enzymatic activity as a consequence [Zeke et al., 2005], but molecular mechanisms of PP5 activation in the living cell are still largely unsolved.

In vivo functions of PP5 have been proposed in several studies through the identification of associating partners, such as heat shock protein 90 (Hsp90), glucocorticoid receptor (GCR), ANP receptor, apoptosis signal kinase 1 (ASK1), ataxia telengiectasia mutated (ATM), and ATM- and Rad3-related (ATR) kinases, and two components of anaphase-promoting complex, CDC16 and CDC27. Taking the biological functions of these interacting proteins into consideration, PP5 is supposed to be involved in a variety of biological signal pathways, including functional modification of molecular chaperons, signal transduction through receptors, mitotic processes, and cell cycle checkpoint [Chen et al., 1996; Ollendorff and Donoghue, 1997; Silverstein et al., 1997]. PP5 is also suspected to be involved in DNA-damage-induced activation of ATM and ATR and oxidative-stress-induced apoptosis signal-regulating kinase 1 (ASK1) inactivation [Morita et al., 2001; Ali et al., 2004; Zhang et al., 2005]. In addition, PP5 associates with microtubule-binding proteins, tau and dynein [Galingniana et al., 2002; Gong et al., 2004], which may indicate the role of PP5 in cytoplasmic molecular transport through the physical interaction with structural proteins, such as tubulin and/or actin. We have recently demonstrated that PP5 localizes at microtubules, and the inhibition of PP5 expression by siRNA in HeLa cells induced abnormal organization of microtubules [Hara et al., our unpublished observation]. Zuo et al. [1998] reported that inhibition of PP5 induces G1 arrest through activation of p53-p21 pathway; however, a detailed molecular mechanism is not clarified yet.

In the present study, we demonstrated an intriguing and novel phenotype caused by the altered expression of the wild-type and mutant PP5. Overexpression of the full-length wild-type PP5 fused with EGFP (EGFP-$PP5_{WT}$) and its phosphatase-dead mutant (EGFP-$PP5_{H304A}$) induced an abnormal nuclear shape in HeLa cells. Furthermore, distinct structural differences were observed between the nuclear shape abnormality induced by wild-type and mutant EGFP-PP5 proteins in terms of the continuity of the nuclear membrane in a cell. For example, overexpression of the former induced multiple nuclei, each of which being demarcated separately by nuclear membrane, but the latter induced clover-like nuclei surrounded by a continuous nuclear membrane, suggesting the presence of two distinct modes of action for PP5 in the induction of abnormal nuclear shapes by its overexpression. A possible and novel role of PP5 is discussed on its involvement in the reconstitution of the nuclear membrane at mitosis.

MATERIALS AND METHODS

Construction of Expression Plasmids with Wild-Type and Phosphatase-Dead Mutants of PP5 and Purification of Those Recombinant PP5 Proteins Expressed in *Escherichia coli*

Prokaryotic expression plasmids for the full-length wild-type rat PP5 fused with glutathione S-transferase (GST) [GST-$PP5_{WT}$] and deletion mutants lacking N-terminal 177 amino acids of PP5 [GST-$PP5C_{WT}$] were constructed as described previously [Fukuda et al., 1996]. An expression plasmid for GST-$PP5C_{H304A}$, harboring an amino acid substitution (His to Ala) at codon 304 in the catalytic domain, was generated by PCR-based site directed mutagenesis, as described previously [Sambrook and Russel, 2001]. GST fusion proteins of PP5 were expressed in *E. coli* and purified, as described previously [Fukuda et al., 1996]. Phosphatase activity of these proteins was determined and the GST-$PP5C_{H304A}$ mutant was later confirmed to be enzymatically inactive.

We also constructed eukaryotic expression vectors for the full-length wild-type rat PP5 fused with EGFP (EGFP-$PP5_{WT}$) and an EGFP-fused deletion mutant of PP5 lacking N-terminal 236 amino acids (EGFP-$PP5C_{WT}$) from the counterpart of each GST-fused proteins. Their phosphatase-dead counterparts, EGFP-$PP5_{H304A}$ and EGFP-$PP5C_{H304A}$, were generated by replacement of the C-terminal catalytic domain from the corresponding counterparts of GST-$PP5_{H304A}$ and GST-$PP5C_{H304A}$.

Cell Culture and Plasmid Transfection

HeLa cells were maintained in Dulbecco's Modified Eagle Medium (DMEM) supplemented with 10% heat-inactivated fetal bovine serum (FBS). For transient transfection of plasmids, cells were seeded at 5×10^4 cells/ml

and transfected with various plasmid DNA, including control pEGFP plasmid, using TransIT reagents (Takara Bio, Inc.) according to the manufacturer's instructions.

Phosphatase Assay

Phosphatase assays using ^{32}P-labeled phosphorylase *a* as a substrate were performed as detailed earlier [MacKintosh and Moorhead, 1993; Fukuda et al., 1996]. The final concentrations of the substrate and GST-PP5 were 0.35 mg/ml and 61 μU/ml, respectively. Phosphatase assays using *p*-nitrophenylphosphate as a substrate were also carried out as described earlier [MacKintosh and Moorhead, 1993] with or without arachidonic acid (Sigma) and okadaic acid (Wako Pure Chemical).

For PP5 proteins expressed in cultured cells, EGFP, EGFP-PP5$_{WT}$, and EGFP-PP5$_{H304A}$ were purified from HeLa cells by immunoprecipitation. Cells, transfected with individual PP5 constructs as described above, were harvested and lysed in a single-detergent lysis buffer composed of 50 mM Tris-HCl (pH 8.0), 150 mM NaCl, 1 mM DTT, 5 mM EDTA, 1% NP-40, 0.1 mM PMSF, and 3 μg/ml leupeptin. The lysate was incubated with anti-GFP antibody (MBL) for 60 min at 4°C and further with protein A sepharose beads for 60 min. The beads were washed extensively by the same buffer three times and PBS twice, and small aliquots of precipitated protein were used for determination of protein content by SDS–PAGE, following silver staining. The remaining beads were divided into three parts and mixed with phosphatase assay buffer. Phosphatase activities of the proteins were measured by the same method as described above.

Establishment of *tet-on* HeLa Cells Expressing PP5 or Phosphatase-Dead Mutants

Expression plasmid pTRE2hyg and HeLa tet-on cells were purchased from Clontech. *Tet-on* HeLa cells were transfected with pTRE2hyg-derivative plasmids, coding either EGFP-PP5$_{WT}$, EGFP-PP5$_{H304A}$, or EGFP. Two days later, the cells were harvested and seeded on 96-well culture plates, and kept propagated for more than 3 weeks. Cell culture was carried out in the presence of G418 (100 ng/ml) and hygromycin B (50 ng/ml). Several clones, which stably express either the wild-type or the phophatase-dead mutant PP5 protein, were isolated. Before conducting further experiments, induction of EGFP-PP5$_{WT}$ and EGFP-PP5$_{H304A}$ proteins were confirmed by the addition of doxycycline (Dox), and cell clones with considerable amounts of PP5 proteins were selected and stored in liquid nitrogen until use.

Immunofluorescence Microscope Observation

After transient transfection of various PP5 constructs, cells were incubated at 37°C for 24 h for further analyses. For *tet-on* HeLa cells, 5×10^4 cells were seeded on culture plates and incubated for another 48 h and subjected to immunocytochemical analysis. For immunofluorescence, cells were fixed with cold methanol for 20 min and incubated in a buffer consisting of 1% BSA-PBS with the first antibody for respective proteins for 60 min, then further incubated with the second antibodies for 60 min at RT or at 4°C. Cells were analyzed under a Zeiss Axiovert 200 fluorescence microscope (Carl Zeiss). Anti-lamin A/C (Chemicon) and B (Oncogene), and Alexa 594 conjugated anti-mouse IgG (Molecular probe) were purchased from each supplier. Counting of cells, possessing deformed nuclei, including di- or multi-nuclei, was carried out by fluorescence images of EGFP or EGFP-PP5 because these proteins localize mainly in cytoplasm and can illustrate the shapes of nuclei. For detailed observation, the images of Hoechst 33342 (Sigma) staining for DNA and immunostaining of lamins were utilized in addition to the EGFP-image.

RESULTS

A Phosphatase-Dead Mutant of PP5 by a Single Amino Acid Substitution

In our previous study and other reports, the N-terminal region containing three TPR motifs, which are suspected to provide a suitable interface for protein–protein interaction [Lamb et al., 1995], inhibits the phosphatase activity of the C-terminal catalytic domain of PP5 [Sinclair et al., 1999; Yang et al., 2005]. The recombinant PP5 protein, GST-PP5C$_{WT}$, containing the rat PP5 from Gly^{178} to Met^{499}, lacking 177 amino acids of the N-terminal, was successfully expressed as a soluble protein in *E. coli* and purified. The purified GST-PP5C$_{WT}$ protein conspicuously showed phosphorylase *a* phosphatase activity (Fig. 1). Amino acid sequence in the catalytic domain of PP5, especially those between cystein at codon 240